行政院國家科學委員會專題研究計畫成果報告

從金屬鏈錯合物到分子金屬導線 (3/3)

計畫類別：☑個別型計畫　□整合型計畫

計畫編號：NSC 89－2119－M－002－009

執行期間：89 年 8 月 1 日至 90 年 8 月 31 日

個別型計畫：計畫主持人：彭旭明
共同主持人：

整合型計畫：總計畫主持人：
子計畫主持人：

註：整合型計畫總報告與子計畫成果報告請分開編印各成一冊，彙整一起繳送國科會。

出席國際學術會議心得報告及發表之論文各一份

處理方式：☑可立即對外提供參考
（請打ｖ）□一年後可對外提供參考
□兩年後可對外提供參考
（必要時，本會得展延發表時限）

執行單位：台灣大學化學系

中華民國　91 年　4 月　29 日

彭旭明

成果報告包括三篇論文：

1. 線形立核鈷錯合物：中性及一個電子氧化之錯合物之合成、結構及物性研究。
2. 非對稱線形立核鎳串錯合物：

   $[Ni_5(tpda)_4(H_2O)(BF_4](BF_4)_2$ 及

   $[Ni_5(tpda)_4(SO_3CF_3)_2](SO_3CF_3)$
3. 線形三核鉻及三核鈷之電化學研究

Report list

1. Linear pentacobalt complexes: synthesis, structures, and physical properties of both neutral and one-electron oxidation compounds, Submitted to *Dalton*.

2. Unsymmetrical linear pentanuclear nickel string complexes: $[Ni_5(tpda)_4(H_2O)(BF_4)](BF4)_2$ and $[Ni_5(tpda)_4(SO_3CF_3)_2](SO_3CF_3)$, Submitted to *Inorg. Chem.*

3. The electrochemical properties of linear thrichromium and tricobalt complexes with bis(2-pyridyl)amido ligands, Submitted to *Dalton*.

Linear pentacobalt complexes: synthesis, structures, and physical properties of both neutral and one-electron oxidation compounds

Chen-Yu Yeh,[a] Chung-Hsien Chou,[a] Kun-Chih Pan,[a] Chih-Chieh Wang,[a] Gene-Hsiang Lee,[a] Y. Oliver Su[a] and Shie-Ming Peng*[ab]

[a] *Department of Chemistry, National Taiwan University, Taipei, Taiwan, ROC. Fax: 886-2-23691487; Tel: 886-2-23630231 ext. 3725; E-mail: smpeng@mail.ch.ntu.edu.tw*
[b] *Institute of Chemistry, Academia Sinica, Taipei, Taiwan, ROC.*

A series of linear pentanuclear cobalt complexes including both neutral and one-electron oxidation forms have been synthesized. The one-electron oxidation products are prepared either by reacting with silver salt or with bulk electrolysis. In all of these complexes the pentacobalt chain adopts a symmetrical arrangement and is helically wrapped by four tpda (the dianion of N,N'-bis(α-pyridyl)- 2,6-diaminopyridine) ligands. Two sets of Co–Co bond distances are observed, in which the average internal (inner) one is about 0.06 Å longer than the external (outer) one. Upon one-electron oxidation, the average Co–Co and Co–N bond distances are not significantly different from those of the neutral analogues whereas the Co–X (X = axial ligand) bond lengths exhibit a slight decrease. All of these complexes show two reversible redox couples at about +0.35 and +0.85 V (vs. Ag/AgCl). The first oxidation is a metal-centered reaction and the product is structurally characterized. The second oxidation product is stable at the time scale of spectroelectrochemistry, but proceeds auto-reduction reaction and forms the corresponding one-electron oxidation product under the crystallization conditions. The NMR results are consistent with the paramagnetism of both neutral and oxidized complexes. The magnetic measurements indicate that the neutral and one-electron oxidation molecules have spin states of S = 1/2 and 1, respectively.

Introduction

The metal-metal interactions in dinuclear complexes have been intensively studied and well understood.[1-4] The multinuclear compounds with oligo-α-pyridylamine as the supporting ligands have received increasing attention because of their versatile chemical and physical properties and the potential application as molecular metal wires since the first reports of the trinuclear copper and nickel complexes bridged by di-α-pyridylamido ligand in 1990-1991.[5,6] In the past decade, a number of tri-,[7-10] tetra,[11] penta-,[12-15] hepta-,[11,16] and nonanuclear[17] metal string complexes have been successfully synthesized and structurally characterized.

In 1994 we reported the first unsymmetrical structure of a tricobalt complex $[Co_3(dpa)_4Cl_2]$ (dpa = the dianion of dipyridylamine), in which the central cobalt ion forms metal–metal bond with one of the two terminal cobalt ions and leaves the other terminal cobalt ion isolated.[7] Three years later, the symmetrical structure of this complex was discovered by Cotton *et al.*[10] Further work by the same group confirmed that both symmetrical and unsymmetrical structures can exist. In this class of linear metal string complexes, both symmetrical and unsymmetrical structures were only found for the molecules with a trichromium,[9] tricobalt, [10] or pentachromium core.[14,15] To see whether or not compounds other than above multinuclear metal complexes can adopt both symmetrical and asymmetrical structures we decided to synthesize the pentacobalt complexes. In our previous brief communication,[12] we described the synthesis, crystal structure, and magnetic properties of $[Co_5(tpda)_4(NCS)_2]$, where tpda is the dianion of N,N'-bis(α-pyridyl)- 2,6-diaminopyridine (tripyridyldiamine, abbreviated by $tpdaH_2$). Unlike the case of $[Co_3(dpa)_4Cl_2]$ that both unsymmetrical and symmetrical structures can exist, the five cobalt atoms in $[Co_5(tpda)_4(NCS)_2]$ can only exist in a symmetrical arrangement. Theoretical calculations show that the bond order between adjacent cobalt atoms is 0.5 with σ character (Figure 1).[13] It is desirable to study how the nature of the axial ligand influences the metal-metal interactions in the pentacobalt compounds. Therefore, a series of $Co_5(tpda)_4(X)_2$ complexes, where X is the axial ligand, were prepared and their crystal structures and physical properties were investigated.

The phenomena of one and two steps spin-crossover have been found in the neutral and one-electron oxidation products, respectively, of linear tricobalt complexes.[7,10] The phenomena of spin-crossover observed in tricobalt complexes prompted us to study if the neutral and one-electron oxidation analogues of the pentanuclear cobalt complexes can undergo spin-crossover process. In addition to the neutral compounds, a series of one-electron oxidation complexes were also synthesized and structurally characterized, and their NMR and magnetic properties were investigated. A comparison was made between the structures and physical properties for the neutral and oxidized complexes. Based on the crystal structures, NMR data and magnetic properties of the neutral and oxidized complexes along with the M.O. calculations, the electronic configuration of the pentacobalt complexes is described.

For clarity, the pentacobalt complexes presented in this paper are listed as follows: $[Co_5(tpda)_4(NCS)_2]$ **(1)**, $[Co_5(tpda)_4Cl_2]$ **(2)**, $[Co_5(tpda)_4(N_3)_2]$ **(3)**, $[Co_5(tpda)_4(CN)_2]$ **(4)**, $[Co_5(tpda)_4(SO_3CF_3)_2]$ **(5)**, $[Co_5(tpda)_4(NCS)_2](ClO_4)$ **(6)**, $[Co_5(tpda)_4Cl_2](ClO_4)$ **(7)**, $[Co_5(tpda)_4(SO_3CF_3)_2](SO_3CF_3)$ **(8)**.

Results and Discussion

Synthesis

We have developed a general method for the synthesis of a series of oligo-α-pyridylamino ligands. The desired ligand, $tpdaH_2$, can be prepared from the reaction of 2,6-diaminopyridine with 2.5 equivalent of 2-chloropyridine in the presence of potassium *t*-butoxide. The reaction of $tpdaH_2$ with $CoCl_2$ in molten naphthalene generated the mononuclear complex *in situ*. The reaction was then followed by the addition of potassium *t*-butoxide in *n*-butanol to give the expected product, $[Co_5(tpda)_4Cl_2]$, with a 10% yield. Under a modified condition, a high yield (42%) for the synthesis of $[Co_5(tpda)_4(NCS)_2]$ was achieved, in which excess NaSCN was added immediately after the addition of potassium *t*-butoxide. The high yielding and reproducible reaction conditions allow us to obtain a large amount of material for ligand exchange and to prepare the oxidized counterparts. The one-electron oxidation products were obtained either by reacting the neutral complexes with silver

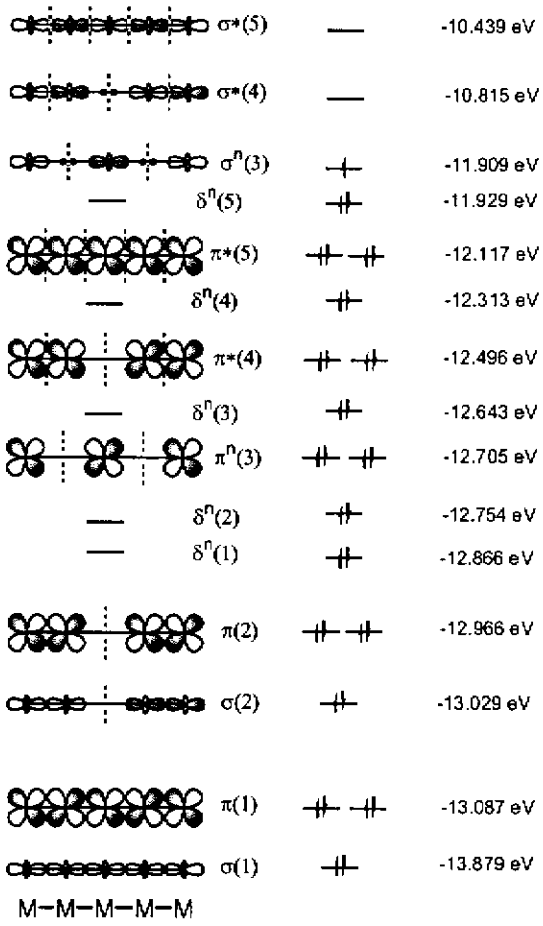

Fig. 1 Qualitative theoretical calculation for $[Co_5(tpda)_4(NCS)_2]$.

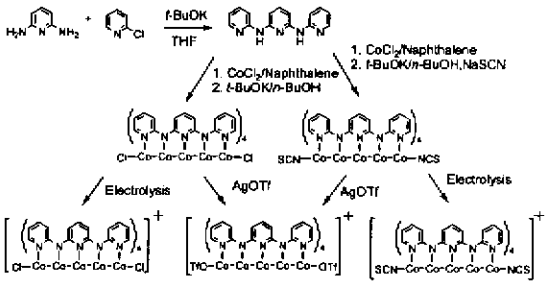

Scheme 1 General route for the preparation of pentadentate ligand N,N'-dipyridyl-2,6-diaminopyridine ($tpdaH_2$) and linear pentanuclear cobalt string complexes.

salts or by bulk electrolysis at $E_{appl.}$ = +0.55 V, which is positive to the formal potential for the first oxidation. The synthesis of the ligand, and the pentanuclear cobalt complexes including both neutral and one-electron oxidation products is outlined in Scheme 1. The spectroscopic data for compounds **1-8** are given in Table 1.

A summary of structural data for compounds **1-5** and **6-8** are listed in Table 2 and 3, respectively. Table 4 gives some selected bond distances for compounds **1-8**. In all these complexes, the pentacobalt chain helically wrapped by four tpda ligands is linear and symmetrical. In compounds **2** and **5**, the molecule resides on a crystallographic site of 2-fold symmetry with the central coblat

Table 1 Spectroscopic data for compounds **1-8**.

	IR (ν/cm^{-1})	UV/Vis/NIR (λ_{max}/nm)	mass (m/z)
1	2060, 1605, 1575, 1548, 1473, 1451	289, 339, 391, 513, 722	1455, 1379
2	1601, 1545, 1470, 1420	294, 331, 351, 524, 752	1409, 1374, 1339
3	2038, 1603, 1575, 1547, 1473, 1452, 1409	294, 327, 375, 527, 730	1423, 1381, 1339
4	2099, 1605, 1575, 1547, 1475, 1452, 1423, 1410	292, 342, 401, 516, 585, 695	1391, 1365, 1339
5	1605, 1579, 1549, 1475, 1455, 1413	286, 308, 380, 514, 794	1637, 1488, 1339
6	2067, 1603, 1577, 1548, 1467, 1424	305, 376, 573, 917	1455, 1397
7	1602, 1577, 1545, 1467, 1424	306, 374, 585, 939	1409, 1374, 1339
8	1603, 1574, 1548, 1469, 1423	302, 373, 547, 958	1637, 1488, 1339

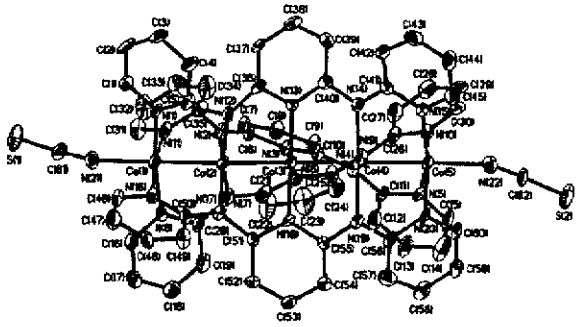

Fig.2 Crystal structure of **1**. Thermal ellipsoids are drawn at the 50% probability level. Hydrogen atoms are omitted for clarity.

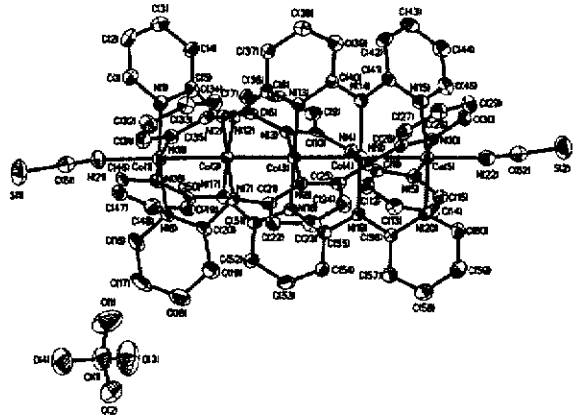

Fig. 3 Crystal structure of **6**. Thermal ellipsoids are drawn at the 50% probability level. Hydrogen atoms are omitted for clarity.

atom on a 2-fold axis perpendicular to the Co_5 chain. The crystal structures of the neutral compounds **1-5** have much in common except that the axial ligands are different. As an example, Figure 2 shows the crystal structure of compound **1**. In the complexes, two types of Co–Co bond distances are observed. The average internal Co–Co bond lengths fall into the range of 2.22–2.24 Å, whereas the external ones range from 2.27 to 2.29 Å. All of the Co–N distances lie in the range of 1.90–1.99 Å. Unlike the case

Table 2 Crystal data for compounds **1-5**

	$1{\cdot}CH_2Cl_2{\cdot}1/2O(C_2H_5)_2{\cdot}1/2H_2O$	$2{\cdot}2CHCl_3{\cdot}O(C_2H_5)_2$	$3{\cdot}2CH_2Cl_2{\cdot}1/3H_2O$	$4{\cdot}3CH_2Cl_2{\cdot}O(C_2H_5)_2$	$5{\cdot}2CH_2Cl_2$
Formula	$C_{65}H_{52}Cl_2Co_5N_{22}S_2O$	$C_{66}H_{56}Cl_6Co_5N_{20}O$	$C_{62}H_{48.67}Cl_4Co_5N_{26}O_{0.33}$	$C_{69}H_{60}Cl_6Co_5N_{22}O$	$C_{64}H_{48}Cl_4Co_5F_6N_{20}O_6S_2$
Formula weight	1586.96	1723.56	1599.72	1720.74	1807.79
Temperature (K)	295 (2)	150(1)	150(1)	150(1)	150(1)
Diffractometer	NONIUS, CAD 4	NONIUS, Kappa CCD	Bruker, SMART	NONIUS, Kappa CCD	NONIUS, Kappa CCD
Wavelength (Å)	0.71073	0.71073	0.71073	0.71073	0.71073
Crystal system	Triclinic	Monoclinic	Rhombohedral	Monoclinic	Monoclinic
Space group	P-1	C2/c	R-3	$P2_1/c$	C2/c
a (Å)	11.802(2)	27.5435(5)	40.3422(11)	21.1260(1)	24.2255(4)
b (Å)	14.631(3)	13.7477(3)	40.3422(11)	16.0070(1)	15.2801(3)
c (Å)	20.184(4)	18.6694(4)	21.0202(6)	22.6729(2)	19.3286(3)
α (°)	73.42(2)	90	90	90	90
β (°)	77.77(2)	99.4304(8)	90	111.6851(4)	103.1489(7)
γ (°)	87.56(2)	90	120	90	90
V (Å^3) / Z	3263.9(11) / 2	6973.8(2) / 4	29626.9(14) / 18	7124.54(8) / 4	6967.2(2) / 4
Absorption Coefficient (mm^{-1})	1.453	1.531	1.460	1.427	1.463
Crystal size (mm)	0.50 × 0.05 × 0.05	0.50 × 0.40 × 0.15	0.48 × 0.12 × 0.10	0.40 × 0.35 × 0.25	0.25 × 0.20 × 0.10
θ range for data collection (°)	1.54 – 22.50	1.93 – 27.50	1.01 – 27.50	1.70 – 27.50	1.73 – 27.50
Reflection collected	8526	38777	89076	106884	24766
Independent reflections	8526 (R_{int} = 0.0000)	7956 (R_{int} = 0.0719)	15139 (R_{int} = 0.0498)	16333 (R_{int} = 0.0620)	8002 (R_{int}= 0.0556)
R_F, R_{wF}^2 (all data)[a]	0.1451, 0.1290	0.1220, 0.2671	0.0792, 0.1861	0.0882, 0.1754	0.1080, 0.2041
R_F, R_{wF}^2 ($I > 2\sigma(I)$)[a]	0.0491, 0.1067	0.0807, 0.2309	0.0537, 0.1644	0.0570, 0.1480	0.0635, 0.1697
GOF	1.001	1.030	1.054	1.046	1.051

[a] $R_F = \Sigma||F_o|-|F_c||/\Sigma|F_o|$; $R_{wF}^2 = [\Sigma w|F_o^2-F_c^2|^2/\Sigma wF_o^4]^{1/2}$

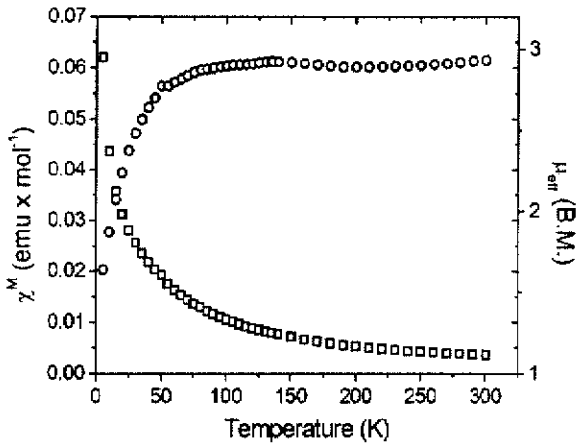

Fig. 4 Temperature-dependent magnetic effective moment (O) and molar magnetic susceptibility (□) for compound **6**.

of $[Co_3(dpa)_4Cl_2]$,[10] in which both symmetrical and unsymmetrical forms can exist, the structure of $[Co_5(tpda)_4X_2]$ can only be observed in the symmetrical form.

It is possible that the identity of the axial ligand could influence the Co–Co and Co–N bond distances. Indeed, the weak nature of the axial ligand $SO_3CF_3^-$ in compound **5** is reflected on both the external Co–Co and Co–N bond distances, which are 0.026 and 0.025 Å shorter, respectively, as compared to those of complex **4**, which has strong axial ligands (CN^-).

The molecular structures of the one-electron oxidation compounds **6-8** are similar to those of the neutral analogues except for the presence of a counter anion to compensate the positive charge on the Co_5 core. Some selected bond distances are listed in Table 4. We expected that some of the interatomic bond distances would be shorter as compared to those in the neutral compounds. However, the Co–N distances for all cobalt atoms remain essentially unchanged upon one-electron oxidation. Moreover, all of the Co–Co bond lengths are slightly longer (by about 0.01–0.02 Å) than those in the neutral analogues. Figure 3 shows the crystal structure of compound **6**.

In the case of tricobalt complexes, the average Co–Cl bond distance in the one-electron oxidation species is 0.15 Å shorter than that of the neutral one.[10] This is a result from removal of one electron from the singly occupied HOMO which has Co–Co nonbonding and Co–Cl antibonding characters as suggested by theoretical calculations.[18] Similar to the case of the tricobalt compounds, theoretical calculations for the pentacobalt complexes reveal that the singly occupied HOMO also has characters of metal-metal nonbonding and metal-ligand antibonding. It was expected that removal of an electron from the HOMO of the neutral complexes resulted in a decrease in Co–Cl bond distances and remained unchanged in Co-Co distances. However, a significant decrease in the Co–X bond distances was not observed upon one-electron oxidation. We believe that the electron cannot be removed from the singly occupied HOMO $\sigma^n(3)$, but from the $\delta^n(5)$ orbital to form a paramagnetic complex with S = 1 as will be discussed later on.

Magnetic Properties

It has been shown that trinuclear cobalt complex $[Co_3(dpa)_4Cl_2]$ undergoes spin-crossover process at temperatures above 160 K.[7,10] Unlike the magnetic properties of $[Co_3(dpa)_4Cl_2]$, the phenomenon of spin-crossover is not observed for the neutral molecules of pentacobalt complexes at temperatures below 300 K. As previously reported, the effective moment of 1.90 μ_B at 300 K for $[Co_5(tpda)_4(NCS)_2]$ is consistent with M.O. calculation as described in Figure 1.[12] Based on the theoretical calculations, the one-electron oxidation products of the pentacobalt complexes should be diamagnetic if the electron is removed from the singly occupied HOMO of the neutral analogues. However, an effective magnetic moment of 0.0 μ_B was not observed for the one-electron oxidation complex at temperatures from 5 to 300 K. The molar magnetic susceptibility (χ^M) and effective magnetic moment (μ_{eff}) of compounds **6** *versus* temperature are presented in Figure 4. The measured μ_{eff} values are essentially constant between 50 and 300 K and follow Curie law with precision. The effective magnetic moment of 2.93 μ_B at 300 K indicates that the complex is paramagnetic and that there are two unpaired electrons in the molecule, even

Table 3 Crystal data for compounds **6-8**

	6	**7**·3CH_2Cl_2	**8**
Formula	$C_{62}H_{44}ClCo_5N_{22}S_2O_4$	$C_{63}H_{50}Cl_6Co_5N_{20}O_4$	$C_{63}H_{44}Co_5F_9N_{22}O_6S_3$
Formula weight	1555.41	1764.93	1787.01
Temperature (K)	150(1)	150(1)	150(1)
Diffractometer	NONIUS, Kappa CCD	NONIUS, Kappa CCD	NONIUS, Kappa CCD
Wavelength (Å)	0.71073	0.71073	0.71073
Crystal system	Orthorhombic	Monoclinic	Monoclinic
Space group	Pbca	Pn	$P2_1$
a (Å)	17.6284(3)	15.6128(2)	13.8809(2)
b (Å)	17.1624(7)	27.9023(5)	17.2756(2)
c (Å)	40.0873(4)	15.8641(3)	13.9058(2)
α (°)	90	90	90
β (°)	90	92.3899(14)	99.7585(4)
γ (°)	90	90	90
V (Å^3) / Z	12128.2(4) / 8	6904.9(2) / 4	3286.37(8) / 2
Absorption Coefficient (mm^{-1})	1.523	1.589	1.433
Crystal size (mm)	0.30 × 0.30 × 0.10	0.40 × 0.27 × 0.02	0.20 × 0.12 × 0.04
θ range for data collection (°)	1.54 –25.00	1.46 –27.50	2.36 –27.50
Reflection collected	27753	44517	48312
Independent reflections	9118 (R_{int} = 0.0647)	26581 (R_{int} = 0.0592)	13837 (R_{int} = 0.0544)
R_F, R_{wF}^2 (all data)[a]	0.0895, 0.1684	0.1170, 0.2241	0.0700, 0.1337
R_F, R_{wF}^2 ($I > 2\sigma(I)$)[a]	0.0581, 0.1444	0.0786, 0.1921	0.0538, 0.1476
GOF	1.149	1.122	1.046

[a] $R_F = \Sigma||F_o|-|F_c||/\Sigma|F_o|$; $R_{wF}^2 = [\Sigma w|F_o^2-F_c^2|^2/\Sigma wF_o^4]^{1/2}$

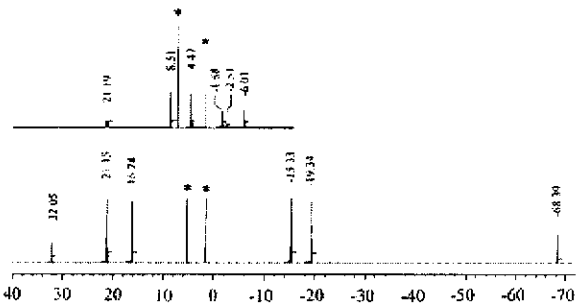

Fig. 5 ^{1}H NMR spectra of compounds **1** (top) and **6** (bottom) in $CDCl_3$ and CD_2Cl_2, respectively, at 20 °C. The starred peaks correspond to the solvent.

though the measured value is slightly higher than the expected (ca. 2.83 μ_B). At temperatures below 50 K, the effective magnetic moment drops sharply as the temperature decreases. This indicates that there are antiferromagnetic interactions in the Co_5 unit. A similar magnetic behavior for one-electron oxidation complexes **7** and **8** with effective moments of 3.18 and 2.86 μ_B, respectively, at 300 K is also observed. On the basis of the magnetic measurements, the electronic configuration of the one-electron oxidation products of $[Co_5(tpda)_4X_2]$ can best be described as the molecules being in a high-spin (S = 1) state where both the $\sigma^n(3)$ and $\delta^n(5)$ orbitals are singly occupied (Figure 1). This literally tell us why the metal-ligand bond distances do not change as significantly as those in the case of trinuclear cobalt complex $[Co_3(dpa)_4Cl_2]$ upon one-electron oxidation.

NMR Spectroscopy

To see whether or not both the neutral and one-electron oxidation compounds of the pentacobalt complexes are paramagnetic as revealed by magnetic measurements, we decided to examine the ^{1}H NMR spectra. Figure 5 shows the ^{1}H NMR spectra of complexes **1** and **6** at room temperature. As expected for paramagnetic complexes, broadened peaks and large chemical shifts of resonance signals were observed for both

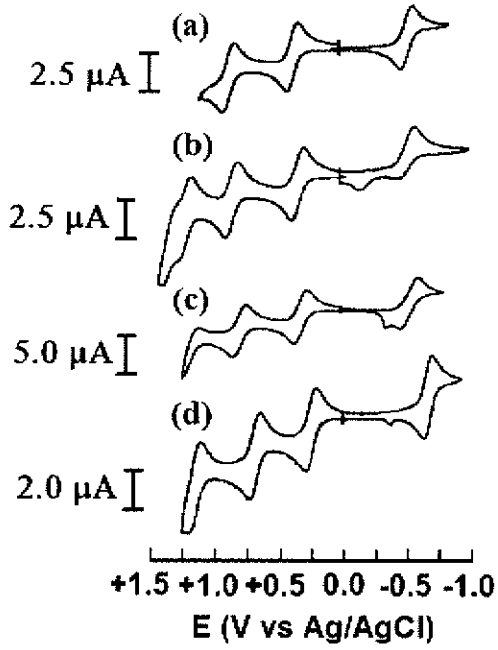

Fig. 6 The cyclic voltammograms of linear pentanuclear string complexes in CH_2Cl_2 containing 0.1 M TBAP. Compounds (a) **1**; (b) **2**; (c) **3**; (d) **4**.

compounds **1** and **6**. For the symmetrical structures of **1** and **6**, there should be only six peaks. Indeed, six lines with intensity ratios, consistent with those expected (i.e., 2:2:2:2:2:1), centered at 21.19, 8.51, 4.47, -1.58, -2.51 and -6.01 ppm were recorded for **1**. The spectrum of **6** also consists of six signals spanning in a larger range, which were found at 32.05, 21.16, 16.24, -15.33, -19.34 and -68.39 ppm with expected intensity ratios. Similar to compounds **1** and **6**, the spectra of both compounds **2** and **7** consist of six signals in similar ranges as those of **1** and **6**, respectively. The ^{1}H NMR spectra of these neutral and one-

Table 4 Selected bond distances for compounds **1-8**

	1	**2**	**3**	**4**	**5**	**6**	**7**	**8**
Co(1)-X[a]	2.076(7)	2.445(2)	2.093(4)	2.024(2)	2.244(3)	2.076(5)	2.416(3)	2.186(4)
Co(5)-X[a]	2.071(8)	2.445(2)	2.089(4)	2.038(4)	2.244(3)	2.037(6)	2.408(3)	2.213(4)
Co(1)-Co(2)	2.276(2)	2.282(1)	2.258(1)	2.279(1)	2.253(1)	2.292(1)	2.300(2)	2.282(1)
Co(2)-Co(3)	2.232(2)	2.235(1)	2.223(1)	2.227(1)	2.225(1)	2.238(1)	2.246(2)	2.253(1)
Co(3)-Co(4)	2.232(2)	2.235(1)	2.221(1)	2.231(1)	2.225(1)	2.243(1)	2.244(2)	2.241(1)
Co(4)-Co(5)	2.271(2)	2.282(1)	2.264(1)	2.286(1)	2.253(1)	2.276(1)	2.285(2)	2.290(1)
Co(1)-N	1.975(7)	1.983(5)	1.972(4)	1.982(3)	1.960(4)	1.973(5)	1.989(8)	1.967(6)
Co(2)-N	1.899(7)	1.914(4)	1.906(4)	1.909(3)	1.914(4)	1.902(4)	1.901(8)	1.884(5)
Co(3)-N	1.930(7)	1.930(4)	1.934(3)	1.932(3)	1.938(4)	1.932(4)	1.926(7)	1.920(5)
Co(4)-N	1.903(7)	1.914(4)	1.922(3)	1.914(3)	1.914(4)	1.900(5)	1.901(8)	1.895(5)
Co(5)-N	1.970(8)	1.983(5)	1.970(4)	1.987(3)	1.960(4)	1.969(5)	1.987(8)	1.961(5)

[a] X = axial ligand.

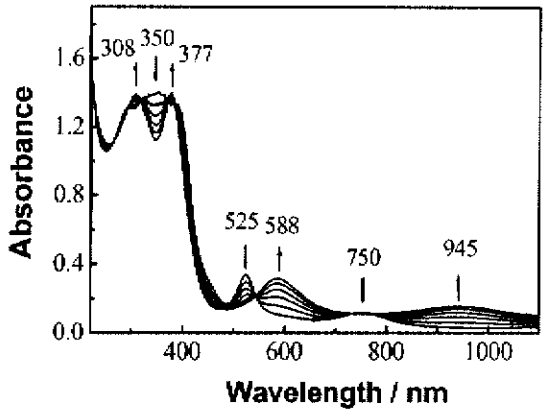

Fig. 7 UV-Vis spectral changes for the first oxidation of compound **1** in CH_2Cl_2 with 0.1 M TBAP at various applied potentials from +0.18 to +0.44 V.

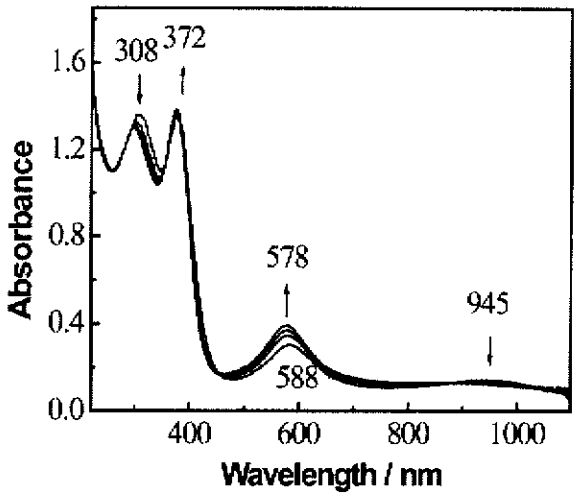

Fig. 8 UV-Vis spectral changes for the second oxidation of compound **1** in CH_2Cl_2 with 0.1 M TBAP at various applied potentials from +0.60 to +1.10 V.

electron oxidation pentanuclear cobalt complexes clearly show the paramagnetism of these compounds in solution at room temperature, even though we are unable to make a straightforward assignment for each of the resonance peaks simply by 1-D ^{1}H NMR. These data are consistent with the fact that the electron is not removed from the singly occupied HOMO $\sigma^*(3)$ of the neutral molecules upon one-electron oxidation.

Electrochemistry

The electrochemistry of compounds **1**, **2**, **3**, and **4** has been carried out. Figure 6 shows their cyclic voltammograms in CH_2Cl_2 containing 0.1 M TBAP. All these complexes exhibit two reversible redox couples at about $E_{1/2}$ = +0.35 and +0.85 V, respectively. Both electrochemical reactions involve one electron transfer as ascertained by spectroelectrochemistry.[19] For compound **2**, another two oxidative waves at potentials of about +1.25 and +1.40 V, which are well resolved by using differential pulse techniques, are observed and each step involves one-electron abstraction as judged by the peak current maximum. The first reduction near -0.50 V is reversible for **1**, and irreversible for **2**, **3**, and **4**. For compound **4**, a small reduction peak near -0.35 V was observed upon the first reduction. This peak progressively increases as the potential is scanned in cycles between 0.00 and -0.75 V, indicating that an absorbed species forms when compound **4** is electrochemically reduced. The electrochemical reductive behavior of **4** and the characterization of the adsorbed species will be published elsewhere.

Figure 7 illustrates spectral changes of compound **2** at applied potentials from +0.18 to +0.44 V in CH_2Cl_2 containing 0.1 M TBAP. The peaks at 350, 525 and 750 nm shift to 308, 377, 588 and 945 nm with clear isosbestic points at 293, 317, 370, 383, 543, 733 and 774 nm. The resulting spectrum is similar to that of the one-electron oxidation products of **2**, obtained by chemical method, suggesting that the oxidation is a metal-centered reaction. Based on the spectral changes of **2** at various applied potentials, the number of electrons transferred is calculated to be one.[19] The one-electron oxidation species of **2** is then characterized as $[Co_5(tpda)_4Cl_2][ClO_4]$, which is further confirmed by the X-ray crystal structure of complex **7**.

The second oxidation was also investigated by spectroelectrochemistry as shown in Figure 8. The peaks at 308, 377, 588 and 945 nm shift to 293, 372 and 578 nm with clear isosbestic points suggesting that no intermediates are produced during the oxidation reactions. The oxidation reaction is reversible. The initial spectrum is restored completely upon re-reduction at +0.55 V. The number of electrons transferred involved in this oxidation reaction is one, which is calculated from the spectral changes at various applied potentials between +0.65 and +1.10 V. The result is consistent with that obtained by cyclic voltammetry. Attempts to isolate and crystallize the two-electron oxidation product were unsuccessful although it was stable at the time scale of spectroelectrochemistry. The two-electron oxidation species undergoes auto-reduction to form the corresponding one-electron oxidation product as evidenced by the UV-Vis spectrum. The spectroelectrochemical behavior of complexes **1**, **3** and **4** is similar to that of **2**. However, the products of the second oxidation are relatively unstable.

Conclusion

This work described the preparation, crystal structures, and the properties of linear pentanuclear cobalt metal string complexes including both neutral and one-electron oxidation compounds. As far as we are aware of, this is the first study on the one-electron oxidation products of the pentacobalt string complexes. Unlike the tricobalt system, all the structures of these complexes in this study are symmetrical and the phenomena of spin-crossover are not observed. The magnetic measurements show that the neutral and one-electron oxidation molecules exhibit spin states of S = 1/2 and 1, respectively. These are consistent with the structural analyses, and rationalized by the qualitative M.O. calculations. Our efforts are currently devoted to the synthesis of multicobalt complexes with a longer chain and self-assembled multinuclear metal string complexes.

Experimental

Materials

All reagents and solvents were obtained from commercial sources and were used without further purification unless otherwise noted. CH_2Cl_2 used for electrochemistry was dried over CaH_2 and freshly distilled prior to use. *n*-BuOH was dried over magnesium turnings and freshly distilled prior to use. Tetra-*n*-butylammonium perchlorate (TBAP) was recrystallized twice from ethyl acetate and further dried under vacuum.

Physical Measurements

Absorption spectra were recorded on a Hewlett Packard model 8453 spectrophotometer. IR spectra were performed with a Nicolet Fourier-Transform IR spectrometer in the range of 500-4000 cm^{-1}. FAB-MS mass spectra were obtained with a JEOL HX-110 HF double focusing spectrometer operating in the positive ion detection mode. Molar magnetic susceptibility was recorded in the range of 5-300 K on s SQUID system with 10,000 Gauss external magnetic field. Electrochemistry was performed with a three-electrode potentiostat (Bioanalytical Systems, Model CV-27) and a BAS X-Y recorder in a CH_2Cl_2 solution deoxygenated by purging with prepuried nitrogen gas. Cyclic voltammetry was conducted with the use of a home-made three-electrode cell equipped with a BAS glassy carbon (0.07 cm^2) or platinum (0.02 cm^2) disk as the working electrode, a platinum wire as the auxiliary electrode, and a home-made Ag/AgCl (sat'd) reference electrode. The reference electrode is separated from the bulk solution by a double junction filled with electrolyte solution. Potentials are reported *vs.* Ag/AgCl (sat'd) and referenced to the ferrocene/ferrocenium (Fc/Fc^+) couple which occurs at $E_{1/2}$ = +0.54 V *vs.* Ag/AgCl (sat'd). The working electrode was polished with 0.03 μm aluminum on Buehler felt pads and was put under ultrasonic for 1 min prior to each experiment. The reproducibility of individual potential values was within ±5 mV. The spectroelectrochemical experiments were accomplished with the use of a 1 mm cuvette, a 100 mesh platinum gauze as working electrode, a platinum wire as auxiliary electrode, and a Ag/AgCl (sat'd) reference electrode.

Preparation of Compounds

$[Co_5(tpda)_4(NCS)_2]$, 1. Ligand $tpdaH_2$ (1.05 g, 4.0 mmole), $CoCl_2$ (0.65 g, 5 mmole) and naphthalene (20 g) were placed in an Erlenmejer flask. Before *t*-BuOK (0.9 g, 8.0 mmole) in *n*-butanol (10 mL) and NaSCN (3.24 g, 40 mmole) was added, the mixture was heated and stirred at 160 °C for 16 hr. The temperature was increased and *n*-butanol was slowly evaporated in a period of 30 min. The resulting solution was then stirred at 220 °C for an additional 30 min. After the mixture was cooled to 80 °C, hexane (100 mL) was added and the precipitate was filtered. The solid was extracted with CH_2Cl_2 and recrystallized from CH_2Cl_2 and methanol to remove the mononuclear complex. Crystallization from CH_2Cl_2 and ether afforded 0.61 g of dark brown crystals (42%). IR (KBr) ν/cm^{-1} = 2060 (C≡N), 1605, 1575, 1548, 1473, 1451 (py); UV/Vis (CH_2Cl_2) λ_{max}/nm (ε/dm^3 mol^{-1} cm^{-1}) = 289 (7.44 × 10^4), 339 (7.94 × 10^4), 391 (7.44 × 10^4), 513 (1.57 × 10^4), 722 (6.01 × 10^3); MS(FAB) m/z 1455 ($[Co_5(tpda)_4(NCS)_2]^-$), 1397 ($[Co_5(tpda)_4NCS]^-$). EA (%) $[Co_5(tpda)_4(NCS)_2]$: calcd. C 51.15, H 3.05, N 21.17; found C 51.29, H 3.10, N 21.78.

$[Co_5(tpda)_4Cl_2]$, 2. Ligand $tpdaH_2$ (1.05 g, 4.0 mmole), $CoCl_2$ (0.65 g, 5 mmole) and naphthalene (20 g) were placed in an Erlenmejer flask. Before *t*-BuOK (0.9 g, 8.0 mmole) in *n*-butanol (10 mL) was added, the mixture was heated and stirred at 160 °C for 16 hr. The temperature was increased and *n*-butanol was slowly evaporated in a period of 30 min. The resulting solution was then stirred at 210 °C for an additional 20 min. After the mixture was cooled to 80 °C, hexane (100 mL) was added and the precipitate was filtered. The solid was extracted with CH_2Cl_2 and recrystallized from CH_2Cl_2 and methanol to remove the mononuclear complex. Crystallization from $CHCl_3$ and ether gave 0.14 g of dark brown crystals (10%). IR (KBr) ν/cm^{-1} = 1601, 1545, 1470, 1420 (py); UV/Vis (CH_2Cl_2) λ_{max}/nm (ε/dm^3 mol^{-1} cm^{-1}) = 294 (7.67 × 10^4), 331 (7.96 × 10^4), 351 (8.12 × 10^4), 524 (1.78 × 10^4), 752 (6.02 × 10^3); MS(FAB) m/z 1409 ($[Co_5(tpda)_4Cl_2]^+$), 1374 ($[Co_5(tpda)_4Cl]^+$), 1339 ($[Co_5(tpda)_4]^+$). EA (%) $[Co_5(tpda)_4Cl_2]$: calcd. C 51.09, H 3.14, N 19.86; found C 50.70, H 3.27, N 19.88.

$[Co_5(tpda)_4(N_3)_2]$, 3. *Method 1:* Ligand $tpdaH_2$ (1.05 g, 4.0 mmole), $CoCl_2$ (0.65 g, 5 mmole) and naphthalene (20 g) were placed in an Erlenmejer flask. After the mixture was stirred at 160 °C for 16 hr, *t*-BuOK (0.9 g, 8.0 mmole) in *n*-butanol (10 mL) was added. NaN_3 (2.60 g, 40 mmole) was then portionwisely added to the mixture. The temperature was increased and *n*-butanol was slowly evaporated in a period of 30 min. The resulting solution was then stirred at 210 °C for an additional 10 min. After the mixture was cooled to 80 °C, hexane (100 mL) was added and the precipitate was filtered. The solid was extracted with CH_2Cl_2 and recrystallized from CH_2Cl_2 and methanol to remove the mononuclear complex. Crystallization from CH_2Cl_2 and ether afforded 0.30 g of dark brown crystals (21%). **CAUTION:** ***NaN_3 is potentially explosive though we have not experienced any problems under the reaction conditions.*** IR (KBr) ν/cm^{-1} = 2038 (N_3), 1603, 1575, 1547, 1473, 1452, 1409 (py); UV/Vis (CH_2Cl_2) λ_{max}/nm (ε/dm^3 mol^{-1} cm^{-1}) = 294 (5.85 × 10^4), 327 (6.10 × 10^4), 375 (6.00 × 10^4), 527 (1.64 × 10^4), 730 (6.49 × 10^3); MS(FAB) m/z 1423 ($[Co_5(tpda)_4(N_3)_2]^+$), 1381 ($[Co_5(tpda)_4N_3]^+$), 1339 ($[Co_5(tpda)_4]^+$). EA (%) $[Co_5(tpda)_4(N_3)_2]\cdot 2CH_2Cl_2$: calcd. C 46.73, H 3.04, N 22.85; found C 46.97, H 3.28, N 23.43.

Method 2: To a solution of $[Co_5(tpda)_4(NCS)_2]$ (140 mg, 0.10 mmole) in CH_2Cl_2 (50 mL) was added $AgClO_4$ (70 mg, 0.33 mmole) in CH_3OH (1 mL). The solution turned from dark brown to bright blue. After stirring for 5 min, the mixture was then filtered. CH_3OH (50 mL) and NaN_3 (320 mg, 50 mmole) were added to the filtrate. The resulting mixture was stirred overnight and then the solid was filtered out. Solvent was removed under reduced pressure. The product was obtained from crystallization by slow diffusion of ether vapor into the solution. Yield: 102 mg, 72%.

$[Co_5(tpda)_4(CN)_2]$, 4. *Method 1:* To a solution of $[Co_5(tpda)_4Cl_2]$ (140 mg, 0.10 mmole) in a mixture of CH_2Cl_2 (50 mL) and CH_3OH (50 mL) was added NaCN (245 mg, 50 mmole). The resulting mixture was stirred overnight and then the solid was filtered out. Solvent was removed under reduced pressure. Crystals were obtained from crystallization by slow diffusion of ether vapor into the solution of the product in CH_2Cl_2. Yield: 120 mg, 86%. IR (KBr) ν/cm^{-1} = 2099 (C≡N),

1605, 1575, 1547, 1475, 1452,1423, 1410 (py); UV/Vis (CH_2Cl_2) λ_{max}/nm (ε/dm^3 mol^{-1} cm^{-1}) = 292 (5.78 × 10^4), 342 (6.55 × 10^4), 401 (4.64 × 10^4), 516 (9.98 × 10^3), 585 (5.49 × 10^3), 695 (6.49 × 10^3); MS(FAB) m/z 1391 ($[Co_5(tpda)_4(CN)_2]^+$), 1365 ($[Co_5(tpda)_4CN]^+$), 1339 ($[Co_5(tpda)_4]^+$). EA (%) $[Co_5(tpda)_4(CN)_2]$: calcd. C 53.50, H 3.17, N 22.14; found C 53.17, H 3.33, N 22.09.

Method 2: A procedure similar to *method 2* for $[Co_5(tpda)_4(N_3)_2]$ was employed except that NaCN instead of NaN_3 was used to give 73% of the product.

$[Co_5(tpda)_4(SO_3CF_3)_2]$, 5. To a solution of $[Co_5(tpda)_4Cl_2]$ (140 mg, 0.10 mmole) in CH_2Cl_2 (50 mL) was added $TlSO_3CF_3$ (177 mg, 0.50 mmole) in CH_3OH (2 mL). The resulting solution was stirred for 2 hr and then filtered. Solvent was removed under reduced pressure. The product was obtained from crystallization by slow diffusion of ether vapor into the solution. Yield: 150 mg, 91%. IR (KBr) ν/cm^{-1} = 1605, 1579, 1549, 1475, 1455,1413 (py); UV/Vis (CH_2Cl_2) λ_{max}/nm (ε/dm^3 mol^{-1} cm^{-1}) = 286 (5.23 × 10^4), 308 (5.36 × 10^4), 380 (5.67 × 10^4), 514 (8.98 × 10^3), 794 (2.64 × 10^3); MS(FAB) m/z 1637 ($[Co_5(tpda)_4(OTf)_2]^+$), 1488 ($[Co_5(tpda)_4OTf]^+$), 1339 ($[Co_5(tpda)_4]^+$). EA (%) $[Co_5(tpda)_4(OTf)_2]$: calcd. C 45.47, H 2.71, N 17.10; found C 45.28, H 2.84, N 17.40.

$[Co_5(tpda)_4(NCS)_2](ClO_4)$, 6. A solution of $[Co_5(tpda)_4(NCS)_2]$ (100 mg) in CH_2Cl_2 (20 mL) containing 0.1 M TBAP was electrolyzed at $E_{appl.}$ = +0.55 V vs Ag/AgCl. The reaction was monitored by UV/Vis spectroscopy. After the reaction was complete, the solution was concentrated under reduced pressure. Deep blue crystals were obtained by slow diffusion of ether vapor into the concentrated CH_2Cl_2 solution. Samples for analysis were crystallized twice from CH_2Cl_2 and ether. Yield: 77 mg (72%). IR (KBr) ν/cm^{-1} = 2067 (C≡N), 1603, 1577, 1548, 1467, 1424 (py); UV/Vis (CH_2Cl_2) λ_{max}/nm (ε/dm^3 mol^{-1} cm^{-1}) = 305 (6.91 × 10^4), 376 (6.70 × 10^4), 573 (1.46 × 10^4), 917 (6.95 × 10^3); MS(FAB) m/z 1455 ($[Co_5(tpda)_4(NCS)_2]^+$), 1397 ($[Co_5(tpda)_4NCS]^+$). EA (%) $[Co_5(tpda)_4(NCS)_2](ClO_4)$: calcd. C 47.88, H 2.85, N 19.81; found C 47.88, H 2.92, N 20.52.

$[Co_5(tpda)_4Cl_2](ClO_4)$, 7. A procedure similar to that for $[Co_5(tpda)_4(NCS)_2](ClO_4)$ was employed except that $[Co_5(tpda)_4Cl_2]$ instead of $[Co_5(tpda)_4(NCS)_2]$ was used to obtain the product. Samples for analysis were crystallized twice from CH_2Cl_2 and ether. Yield: 78 mg (73%). IR (KBr) ν/cm^{-1} = 1602, 1577, 1545, 1467, 1424 (py); UV/Vis (CH_2Cl_2) λ_{max}/nm (ε/dm^3 mol^{-1} cm^{-1}) = 306 (7.36 × 10^4), 374 (7.31 × 10^4), 585 (1.44 × 10^4), 939 (6.85 × 10^3); MS(FAB) m/z 1409 ($[Co_5(tpda)_4Cl_2]^+$), 1374 ($[Co_5(tpda)_4Cl]^+$), 1339 ($[Co_5(tpda)_4Cl]^+$). EA (%) $[Co_5(tpda)_4Cl_2](ClO_4)$: calcd. C 47.72, H 2.94, N 18.55; found C 47.46, H 3.05, N 19.06.

$[Co_5(tpda)_4(OTf)_2](OTf)$, 8. To a solution of $[Co_5(tpda)_4(NCS)_2]$ (145 mg, 0.10 mmol) in CH_2Cl_2 (50 ml) was added AgOTf (103 mg, 0.40 mmol) in CH_3OH (1 mL). The resulting mixture was stirred for 5 min. The solution turned from dark brown to bright blue. After the solution was filtered solvent was removed under reduced pressure. The blue solid was dissolved in a mixture of CH_2Cl_2 and CH_3OH, and crystallized by slow diffusion of ether vapor into the solution to give dark blue crystals with a 52% yield (93 mg). IR (KBr) ν/cm^{-1} = 1603, 1574, 1548, 1469, 1423 (py); UV/Vis (CH_2Cl_2) λ_{max}/nm (ε/dm^3 mol^{-1} cm^{-1}) = 302 (1.26 × 10^5), 373 (1.29 × 10^5), 574 (2.11 × 10^4), 958 (8.58 × 10^3); MS(FAB) m/z 1637 ($[Co_5(tpda)_4(OTf)_2]^+$), 1488 ($[Co_5(tpda)_4(OTf)]^+$), 1339 ($[Co_5(tpda)_4]^+$). EA (%) $[Co_5(tpda)_4(OTf)_2](OTf)$: calcd. C 42.34, H 2.48, N 15.68; found C 42.17, H 2.57, N 16.00.

Crystal Structure Determinations

The chosen crystals were mounted on a glass fiber. Data collection was carried out on a NONIUS CAD4 diffractometer for **1** and on a BRUKER SMART CCD for **3** with Mo radiation (λ = 0.71073 Å). Cell parameters were retrieved and refined using the CAD4 software[20] on 25 reflections for **1** and the *SAINT* software[21] on all reflections for **3**. Data reduction was performed on the *NRCSDP*[22] and *SAINT*[21] software for **1** and **3**, respectively. An empirical absorption was based on the symmetry-equivalent reflections and absorption corrections were applied with the *PSI-SCAN* and *SADABS*[23] programs, respectively. Data collection for **2**, **4**, **5**, **6**, **7**, and **8** was carried out on a NONIUS Kappa CCD diffractometer. Cell parameters were retrieved and refined using *DENZO-SMN* software on all observed reflections.[24] Data reduction was performed with the *DENZO-SMN* software.[24] An empirical absorption was based on the symmetry-equivalent reflections and absorption corrections were applied with the SORTAV program.[25] All the structures were solved by using the *SHELXS-97*[26] and refined with *SHELXL-97*[27] by full-matrix least squares on F^2 values. Hydrogen atoms were fixed at calculated positions and refined using a riding mode. The detailed crystal data are listed in Tables 2 and 3.

Acknowledgment

The authors acknowledge the National Science Council of Taiwan for financial support.

References

1 F. A. Cotton and R. A. Walton, in *Multiple Bonds Between Metal Atoms*, 2nd ed., Clarendon Press, Oxford, U. K., 1993.

2 F. A. Cotton and G. Wilkinson, in *Advanced Inorganic Chemistry*, 5th ed., Wiley, New York, 1988; Chapter 23.

3 G. Aullon, P. Alemany and S. Alvarez, *Inorg. Chem.*, 1996, **35**, 5061.

4 F. Mota, J. J. Novoa, J. Losada, S. Alvarez, R. Hoffmann and J. Silversgtre, *J. Am. Chem. Soc.*, 1993, **115**, 6216; J. Losada, S. Alvarez, J. J. Novoa, F. Mota, R. Hoffmann and J. Silverstre, *J. Am. Chem. Soc.*, 1990, **112**, 8998.

5 S. Aduldecha and B. Hathaway, *J. Chem. Soc., Dalton. Trans.*, 1991, 993.

6 G. J. Pyrka, M. El-Mekki and A. A. Pinkerton, *J. Chem. Soc., Chem. Commun.*, 1991, 84; L.-P. Wu, P. Field, T. Morrissey, C. Murphy, P. Nagle, B. Hathaway, C. Simmons and P. Thornton, *J. Chem. Soc., Dalton. Trans.*, 1990, 3835.

7 E.-C. Yang, M.-C. Cheng, M.-S. Tsai and S.-M. Peng, *J. Chem. Soc., Chem. Commun.*, 1994, 2377; J.-T. Sheu, C.-C. Lin, I. Chao, C.-C. Wang and S.-M. Peng, *Chem. Commun.*, 1996, 315.

8 R. Clérac, F. A. Cotton, K. R. Dunbar, C. A. Murillo, I. Pascual and X. Wang, *Inorg. Chem.*, 1999, **38**, 2655; F. A. Cotton, L. M. Daniels, P. Lei, C. A. Murillo and X. Wang, *Inorg. Chem.*, 2001, **40**, 2778; R. Clérac, F. A. Cotton, L. M. Daniels, J. Gu, C. A. Murillo and H.-C. Zhou, *Inorg. Chem.*, 2000, **39**, 4488.

9 F. A. Cotton, L. M. Daniels, C. A. Murillo and I. Pascual, *J. Am. Chem. Soc.*, 1997, **119**, 10223; F. A. Cotton, L. M. Daniels, C. A. Murillo and I. Pascual, *Inorg. Chem. Commun.*, 1998, 1, 1; R. Clérac, F. A. Cotton, L. M. Danniels, K. R. Dunbar, C. A. Murillo and I. Pascual, *Inorg. Chem.*, 2000, **39**, 748; R. Clérac, F. A. Cotton, L. M. Daniels, K. R. Dunbar, C. A. Murillo and I. Pascual, *Inorg. Chem.*, 2000, **39**, 752; R. Clérac, F. A. Cotton, L. M. Daniels, K. R. Dunbar, C. A. Murillo and H.-C. Zhou, *Inorg. Chem.*, 2000, **39**, 3414.

10 F. A. Cotton, L. M. Daniels and G. T. Jordan IV, *Chem. Commun.*, 1997, 421; F. A. Cotton, L. M. Daniels, G. T. Jordan IV and C. A. Murillo, *J. Am. Chem. Soc.*, 1997, **119**, 10377; F. A. Cotton, C. A. Murillo and X. Wang, *Inorg. Chem.*, 1999, **38**, 6294; F. A. Cotton, C. A. Murillo and X. Wang, *J. Chem. Soc., Dalton Trans.*, 1999, 3327; R. Clérac, F. A. Cotton, L. M. Daniels, K. R. Dunbar, T. Lu, C. A. Murillo and X. Wang, *J. Am. Chem. Soc.*, 2000, **122**, 2272; R. Clérac, F. A. Cotton, K. R. Dunbar, T. Lu, C. A. Murillo and X. Wang, *Inorg. Chem.*, 2000, **39**, 3065; R. Clérac, F. A. Cotton, L. M. Daniels, K. R. Dunbar, K. Kirschbaum, C. A. Murillo, A. A. Pinkerton, A. J. Schultz and X. Wang, *J. Am. Chem. Soc.*, 2000, **122**, 6226; R. Clérac, F. A. Cotton, L. M. Daniels, K. R. Dunbar, C. A. Murillo and X. Wang, *J. Chem. Soc., Dalton Trans.*, 2001, 386; R. Clérac, F. A. Cotton, L. M. Daniels, K. R. Dunbar, C. A. Murillo

and X. Wang, *J. Am. Chem. Soc.*, 2001, **123**, 1256; R. Clérac, F. A. Cotton, S. P. Jeffery, C. A. Murillo and X. Wang, *J. Am. Chem. Soc.*, 2001, **123**, 1265.

11 S.-Y. Lai, T.-W. Lin, Y.-H. Chen, C.-C. Wang, G.-H. Lee, M.-H. Yang, M.-K. Leung and S.-M. Peng, *J. Am. Chem. Soc.*, 1999, **121**, 250; S.-Y. Lai, C.-C. Wang, Y.-H. Chen, C.-C. Lee, Y.-H. Liu and S.-M. Peng, *J. Chin. Chem. Soc.*, 1999, **46**, 477.

12 S.-J. Shieh, C.-C. Chou, G.-H. Lee, C.-C. Wang and S.-M. Peng, *Angwe. Chem. Int. Ed. Engl.*, 1997, **36**, 56.

13 C.-C. Wang, W.-C. Lo, C.-C. Chou, G.-H. Lee, J.-M. Chen and S.-M. Peng, *Inorg. Chem.*, 1998, **37**, 4059.

14 H.-C. Chang, J.-T. Li, C.-C. Wang, T.-W. Lin, H.-C. Lee, G.-H. Lee and S.-M. Peng, *Eur. J. Inorg. Chem.*, 1999, 1243.

15 F. A. Cotton, L. M. Daniels, C. A. Murillo and X. Wang, *Chem. Commun.*, 1999, 2461; F. A. Cotton, L. M. Daniels, C. A. Murillo and X. Wang, J. *Chem. Soc., Dalton Trans.*, 1999, 517.

16 Y.-H. Chen, C.-C. Lee, C.- C. Wang, G.- H. Lee, S.-Y. Lai, F.-Y. Li, C.-Y. Mou, S.-M. Peng, *Chem. Commun.*, 1999, 1667.

17 S.-M. Peng, C.-C. Wang, Y.-L. Jang, Y.-H. Chen, F.-Y. Li, C.-Y. Mou and M.-K. Leung, *J. Magn. Magn. Mater.*, 2000, **209**, 80.

18 M.-M. Rohmer and M. Benard, *J. Am. Chem. Soc.*, 1998, **120**, 9372.

19 D. F. Rohrbach, E. Deutsch, W. R. Heineman and R. F. Pasternack, *Inorg. Chem.* 1977, **16**, 2650.

20 Enraf-Nonius, *CAD4 software, version 5.0*, Enraf-Nonius, Deft, Netherland, 1989.

21 *SAINT V 6.02 Software for the CCD Detector Integration*, Brucker Analytical Instruments Division, Madison, WI, 1997.

22 E. J. Gabe, Y. Lepage, J. P. Charpand, F. L. Lee and P. S. White, *J. Appl. Cryst.*, 1989, **22**, 384.

23 G. M. Sheldrick, *SADABS, Program for Bruker Area Detector Absorption Correction*, University of Göttingen, Germany, 1997.

24 Z. Otwinowski and W. Minor, *Processing of X-ray Diffraction Data Collected in Oscillation Mode*, Methods in Enzymology, Volume **276**: Macromolecular Crystallography, part A; Carter, C. W., Sweet Jr. & R. M., Eds., Academic Press, 1997.

25 R. H. Blessing, *Acta. Cryst.*, 1995, **A51**, 33.

26 G. M. Sheldrick, *Acta. Cryst.*, 1990, **A46**, 467.

27 G. M. Sheldrick, *SHELXL-97, Program for the Refinement of Crystal Structures*, University of Göttingen, Germany, 1997.

Synopsis

Linear pentacobalt complexes: synthesis, structures, and physical properties of both neutral and one-electron oxidation compounds

Chen-Yu Yeh, Chung-Hsien Chou, Kun-Chih Pan, Chih-Chieh Wang, Gene-Hsiang Lee, Y. Oliver Su and Shie-Ming Peng*

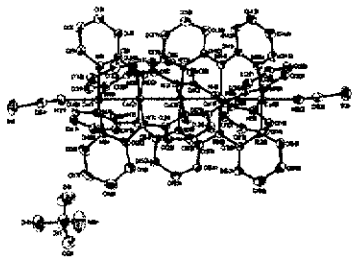

Both neutral and one-electron oxidation compounds of linear pentanuclear cobalt complexes are prepared and structurally characterized, and their structures are compared.

Unsymmetrical Linear Pentanuclear Nickel String Complexes: $[Ni_5(tpda)_4(H_2O)(BF_4)](BF_4)_2$ and $[Ni_5(tpda)_4(SO_3CF_3)_2](SO_3CF_3)$

Chen-Yu Yeh,[†] Yi-Li Chiang,[†] Gene-Hsiang Lee[†] and Shie-Ming Peng*[,†,‡]

Department of Chemistry, National Taiwan University, Taipei, Taiwan, and Institute of Chemistry, Academia Sinica, Taipei, Taiwan

* Author to whom correspondence should be addressed. E-mail: smpeng@mail.ch.ntu.edu.tw

[†] National Taiwan University

[‡] Academia Sinica

RECEIVED DATE (will be automatically inserted after manuscript is accepted)

The one-electron oxidized linear pentanuclear nickel complexes $[Ni_5(tpda)_4(H_2O)(BF_4)](BF_4)_2$ (**1**) and $[Ni_5(tpda)_4(SO_3CF_3)_2](SO_3CF_3)$ (**2**) have been synthesized by reacting the neutral compound $[Ni_5(tpda)_4Cl_2]$ with the corresponding silver salts. These compounds have been characterized by various spectroscopic techniques. Compound **1** crystallizes in the monoclinic space group $P2_1/n$ with a = 15.3022(1) Å, b = 31.0705(3) Å, c = 15.8109(2) Å, β = 92.2425(4)°, V = 7511.49(13) Å^3, Z = 4, and compound **2** in the monoclinic space group $C2/c$ with a = 42.1894(7) Å, b = 17.0770(3) Å, c = 21.2117(4) Å, β = 102.5688(8)°, V = 14916.1(5) Å^3, Z = 8. X-ray structural studies reveal an unsymmetrical Ni_5 unit for both compound **1** and **2**. Compounds **1** and **2** show stronger Ni–Ni interactions as compared to the neutral compounds.

Much attention has been paid to linear multinuclear metal string complexes due to their attractive properties such as strong metal-metal interactions in the molecules and their potential to be applied as molecular electronics.[1-12] A number of multinuclear metal string complexes have been prepared and structurally characterized since the first reports of the trinuclear copper and nickel complexes bridged by di-2-pyridylamido ligand (dpa) in 1990–1991.[1,2] Previous reports showed that there are no metal-metal bonds in the neutral form of tri-, penta-, hepta-, and nonanuclear nickel complexes.[3,4] In these multinuclear nickel complexes, all the internal nickel ions are in a low-spin state, whereas the two external nickel ions are in a high spin-state with S = 1. The antiferromagnetic coupling constants between the two terminal nickel ions are -99, -8.3, -3.8, and -1.7 cm^{-1} for the tri-, penta-, hepta-, and nonanickel dichloride complexes, respectively.[4] To see whether or not the metal-metal interactions and the structures can be influenced upon oxidation, we decided to synthesize the one-electron oxidation counterparts of the linear pentanuclear nickel string complexes. We report here the synthesis and the unusual unsymmetrical structures of the linear one-electron oxidation pentanuclear string complexes, $[Ni_5(tpda)_4(H_2O)(BF_4)](BF_4)_2$ (**1**) and $[Ni_5(tpda)_4(SO_3CF_3)_2](SO_3CF_3)$ (**2**) ($tpdaH_2$ = tripyridyldiamine), along with their magnetic properties. To the best of our knowledge, compounds **1** and **2** are the first linear multinickel complexes with an unsymmetrical structure.

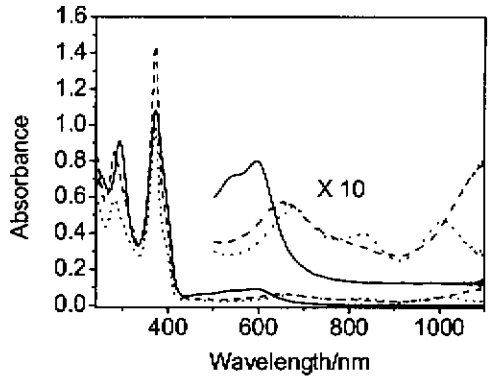

Figure 1. UV-Vis spectra of (a) $[Ni_5(tpda)_4Cl_2]$ (solid line); (b) **1** (dash line); (c) **2** (dot line) in CH_2Cl_2. Concentration: 1.0×10^{-5} M.

The one-electron oxidation of the pentanuclear nickel complexes were achieved by the reaction of excess silver salts and $[Ni_5(tpda)_4Cl_2]$ (**3**). Two one-electron oxidation products, **1** and **2**, were obtained and characterized by various spectroscopic methods such as mass, UV-Vis, IR, and X-ray diffraction. The UV/Vis/Near IR spectra of complexes **1** and **2** showed significant differences from that of the neutral compound, $[Ni_5(tpda)_4Cl_2]$. As shown in Figure 1, upon one-electron oxidation the peaks for $[Ni_5(tpda)_4Cl_2]$ at 292, 373, 480, 548, and 594 nm shifted to 281, 372, 652, and 1150 nm for **1**, and 282, 372, 669, 832, and 1010 nm for **2**.

The most unambiguous confirmation for compounds **1** and **2** is from the X-ray crystal structures. Some selected

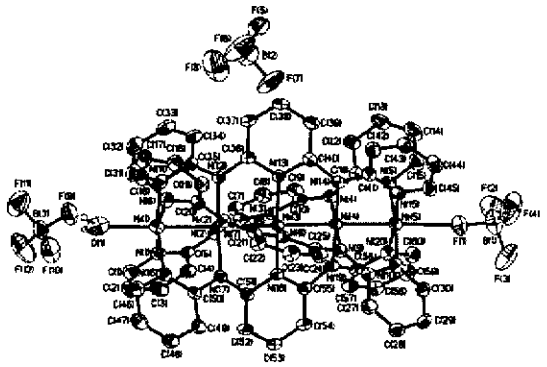

Figure 2. Crystal Structure of compound **1**. Atoms are drawn at the 30% probability level and hydrogen atoms are omitted for clarity.

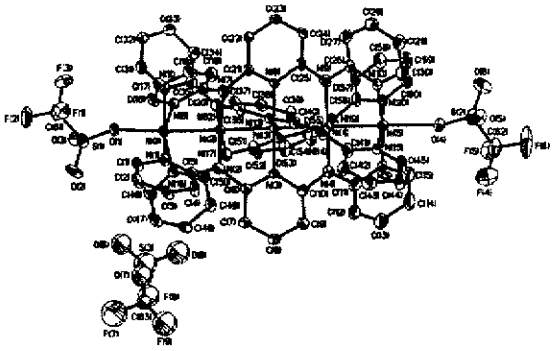

Figure 3. Crystal Structure of compound **2**. Atoms are drawn at the 30% probability level and hydrogen atoms are omitted for clarity.

bond distances for **1**, **2**, **3**, and $[Co_5(tpda)_4(NCS)_2]$ (**4**) are given in Table 1.[13] In compound **1**, five nickel ions are helically supported by four $tpda^{2-}$ ligands in a spiral configuration and essentially form a linear arrangement as shown in Figure 2. The axial ligands are provided by a BF_4^- anion and a H_2O molecule. The two positive charges in the Ni_5 core are compensated by two BF_4^- anions. The axial H_2O ligand forms H-bonding with one of the BF_4^- ions, in which the O(1)–F(5) distance is 2.704 Å. The nickel–axial ligand bond distances are 2.255(6) and 2.470(4) Å for Ni(1)–O(1) and Ni(5)–F(1), respectively. The most striking feature in the crystal structure of **1** is that the Ni_5 chain of the molecule adopts an unsymmetrical structure with Ni–Ni distances of 2.337(1), 2.261(1), 2.245(1), and 2.300(1) Å for Ni(1)–Ni(2), Ni(2)–Ni(3), Ni(3)–Ni(4), Ni(4)–Ni(5), respectively. Compared to the Ni–Ni bond lengths in **3**, both the internal and external Ni–Ni bond distances in compounds **1** and **2** are shorter by 0.04–0.08 Å. Unlike the case of compound **3** where the Ni–N distances for the terminal Ni ions are considerably longer than those for the internal Ni ions, the average Ni–N distances in **1** are 2.023(5), 1.895(5), 1.911(5), 1.892(5), and 1.929(5) Å for Ni(1), Ni(2), Ni(3), Ni(4) and Ni(5), respectively. These results indicate that Ni(1) is in a high-spin state while the other four Ni ions are in a low-spin state, and the one-electron oxidation occurs at the terminal Ni(5) ion. However, we cannot rule out the possibility of the positive

Table1. Selected bond distances for **1**, **2**, **3**, and **4**.

	1	**2**	**3**	**4**
M(1)-X[a]	2.255(6)	2.059(7)	2.346(3)	2.07(1)
M(5)-Y[a]	2.470(4)	2.338(8)	2.346(3)	2.06(1)
M(1)-M(2)	2.337(1)	2.358(2)	2.385(2)	2.281(3)
M(2)-M(3)	2.261(1)	2.276(2)	2.306(1)	2.236(3)
M(3)-M(4)	2.245(1)	2.245(2)	2.306(1)	2.233(3)
M(4)-M(5)	2.300(1)	2.304(1)	2.385(2)	2.277(3)
M(1)-N	2.023(5)	2.081(10)	2.111(9)	1.96(1)
M(2)-N	1.895(5)	1.874(10)	1.90(2)	1.90(1)
M(3)-N	1.911(9)	1.904(9)	1.904(8)	1.93(1)
M(4)-N	1.892(5)	1.885(11)	1.90(2)	1.90(1)
M(5)-N	1.929(5)	1.948(9)	2.111(9)	1.96(1)

[a] X, Y = axial ligands. X = H_2O, Y = BF_4^- for **1**; X = Y = $CF_3SO_3^-$ for **2**; X = Y = Cl^- for **3**; X = Y = NCS^-, M = Co^{II} for **4**.

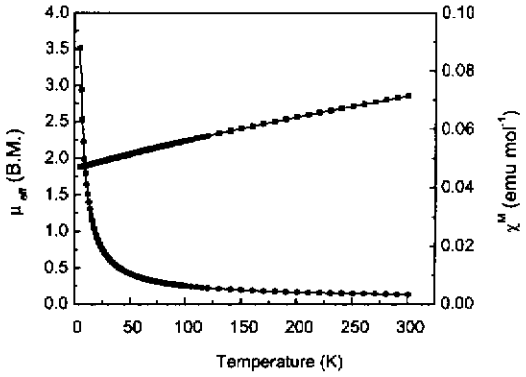

Figure 4. Temperature-dependent magnetic effective moment (□) and molar magnetic susceptibility (○) for compound **1**. Solid lines represent fitting of the experimental data.

charge being delocalized in the four low-spin nickel ions.

It has been found that trinuclear cobalt and chromium complexes exhibit both symmetrical and unsymmetrical structures depending on the nature of the axial ligands,[4] the crystal environment,[5,9] and the oxidation states.[4,10] The unsymmetrical structure of compound **1** might be induced by the different nature of the axial ligands, BF_4^- and H_2O, or by the different Ni–Ni interactions occurring in the molecule. However, the possibility of being induced by the different nature of the axial ligands should be ruled out as evidenced by the crystal structure of **2**, in which the two axial ligands are the same (Figure 3). Compared to **1**, the extent of asymmetry of compound **2** is even more pronounced as judged from the unsymmetrical Ni–Ni bond distances of 2.358(2), 2.276(2), 2.245(2), and 2.304(2) Å. The significant differences between the two terminal nickel ions can also be viewed from the different metal–ligand bond distances of 2.059(7) and 2.338(8) Å for Ni(1)–O(1) and Ni(5)–O(4), respectively. The average Ni–N lengths are not significantly different from those in compound **1** as shown in Table 1. According to the structural analyses, the electronic configuration of **2** can be considered identical with that of **1**.

Theoretical calculations show that there are no metal–metal bonds in the neutral molecules of the pentanickel

complexes and the bond order for Co–Co in neutral pentacobalt complexes is estimated to be 0.5.[4b] Comparing compounds **1** and **2** to **3** and **4**, the Ni–Ni bond distances are in between the corresponding metal–metal distances in **3** and **4**. We believe that considerable unsymmetrical Ni–Ni bonding interactions, especially, on the Ni(5) site exist in **1** and **2**.

The measured effective magnetic moment μ_{eff} and the molar magnetic susceptibility χ^M of compound **2** with respect to temperatures are given in Figure 4. The experimental data obtained are close to the simulated values (solid lines).[14] At the temperatures measured, the effective magnetic moment μ_{eff} of 1.87 μ_B at 5 K increase gradually to a value of 2.86 μ_B at 300 K without reaching saturation. The effective magnetic moment at room temperature is smaller than the estimated value of 3.32 μ_B (two independent spins of S = 1 and S = 1/2). The magnetic data suggest that the terminal Ni(1) ion with S = 1 is antiferromagnetically coupled with the terminal Ni(5) ion with S = 1/2 or the remaining Ni_4 unit with a delocalized unpaired electron. The coupling constants of the antiferromagnetic interactions in the pentanickel core are estimated to be -555 and -318 cm^{-1} for **1** and **2**, respectively, which are much higher than those for **3** (-8.3 cm^{-1}) and $[Ni_3(dpa)_4Cl_2]$ (-99 cm^{-1}), indicating that there are strong metal–metal interactions in these oxidized complexes. The magnetic results are in agreement with the X-ray crystal structural analyses.

In summary, the one-electron oxidation products of the pentanuclear nickel string complexes have been successfully synthesized. The unusual unsymmetrical structures of these oxidized complexes are proven by X-ray crystal structure analysis. One of the terminal nickel ion (Ni(1)) can be regarded as being in a high-spin state with S = 1 while the other four nickel ions are in a low-spin state with a localized (on Ni(5)) or delocalized electron. The differences in the metal-metal interactions between the neutral and one-electron oxidation complexes might shed light on the application of these molecules as "molecular switches". The studies on the conductivity of both the neutral and one-electron oxidation complexes using SAM techniques are currently underway in our laboratory.

Acknowledgment. The authors acknowledge the National Science Council and the Ministry of Education of Taiwan for financial support.

Supporting Information Available: Synthetic procedure and characterization for compounds **1** and **2**, and crystallographic data in CIF format. This material is available free of charge via the Internet at http://pubs.acs.org.

(1) Aduldecha, S.; Hathaway, B. *J. Chem. Soc., Dalton. Trans.*, **1991**, 993.
(2) (a) Pyrka, G. J.; El-Mekki, M.; Pinkerton A. A. *J. Chem. Soc., Chem. Commun.*, **1991**, 84. (b) Wu, L.-P.; Field, P.; Morrissey, T.; Murphy, C.; Nagle, P.; Hathaway, B.; Simmons, C.; Thornton, P. *J. Chem. Soc., Dalton. Trans.*, **1990**, 3835.
(3) Clérac, R.; Cotton, F. A.; Dunbar, K. R.; Murillo, C. A.; Pascual, I.; Wang, X. *Inorg. Chem.* **1999**, *38*, 2655.
(4) (a) Shieh, S.-J.; Chou, C.-C.; Lee, G.-H.; Wang, C.-C.; Peng, S.-M. *Angwe. Chem. Int. Ed. Engl.* **1997**, *36*, 56. (b) Wang, C.-C.; Lo, W.-C.; Chou, C.-C.; Lee, G.-H.; Chen, J.-M.; Peng, S.-M. *Inorg. Chem.* **1998**, *37*, 4059. (c) Lai, S.-Y.; Lin, T.-W.; Chen, Y.-H.; Wang, C.-C.; Lee, G.-H.; Yang, M.-H.; Leung, M.-K.; Peng, S.-M. *J. Am. Chem. Soc.* **1999**, *121*, 250. (d) Lai, S.-Y.; Wang, C.-C.; Chen, Y.-H.; Lee, C.-C.; Liu, Y.-H.; Peng, S.-M. *J. Chin. Chem. Soc.* **1999**, *46*, 477. (e) Peng, S.-M.; Wang, C.-C.; Jang, Y.-L.; Chen, Y.-H.; Li, F.-Y.; Mou, C.-Y.; Leung, M.-K. *J. Magn. Magn. Mater.* **2000**, *209*, 80.
(5) (a) Yang, E.-C.; Cheng, M.-C.; Tsai, M.-S.; Peng, S.-M. *J. Chem. Soc., Chem. Commun.*, **1994**, 2377. (b) Sheu, J.-T.; Lin, C.-C; Chao, I.; Wang, C.-C.; Peng, S.-M. *Chem. Commun.* **1996**, 315.
(6) Cotton, F. A.; Daniels, L. M.; Lei, P.; Murillo, C. A.; Wang, X. *Inorg. Chem.* **2001**, *40*, 2778. (c) Clérac, R.; Cotton, F. A.; Daniels, L. M.; Gu. J.; Murillo, C. A.; Zhou, H.-C. *Inorg. Chem.* **2000**, *39*, 4488.
(7) (a) Cotton, F. A.; Daniels, L. M.; Murillo, C. A.; Pascual, I. *J. Am. Chem. Soc.* **1997**, *119*, 10223. (b) Cotton, F. A.; Daniels, L. M.; Murillo, C. A.; Pascual, I. *Inorg. Chem. Commun.* **1998**, *1*, 1. (c) Clérac, R.; Cotton, F. A.; Danniels, L. M.; Dunbar, K. R.; Murillo, C. A.; Pascual, I. *Inorg. Chem.* **2000**, *39*, 748. (d) Clérac, R.; Cotton, F. A.; Daniels, L. M.; Dunbar, K. R.; Murillo, C. A.; Pascual, I. *Inorg. Chem.* **2000**, *39*, 752. (e) Clérac, R.; Cotton, F. A.; Daniels, L. M.; Dunbar, K. R.; Murillo, C. A.; Zhou, H.-C. *Inorg. Chem.* **2000**, *39*, 3414.
(8) (a) Cotton, F. A.; Daniels, L. M.; Jordan IV, G. T. *Chem. Commun.* **1997**, 421. (b) Cotton, F. A.; Daniels, L. M.; Jordan IV, G. T.; Murillo, C. A. *J. Am. Chem. Soc.* **1997**, *119*, 10377. (c) Cotton, F. A.; Murillo, C. A.; Wang, X. *Inorg. Chem.* **1999**, *38*, 6294. (d) Cotton, F. A.; Murillo, C. A.; Wang, X. *J. Chem. Soc., Dalton Trans.*, **1999**, 3327. (e) Clérac, R.; Cotton, F. A.; Daniels, L. M.; Dunbar, K. R.; Lu, T.; Murillo, C. A.; Wang, X. *J. Am. Chem. Soc.* **2000**, *122*, 2272. (f) Clérac, R.; Cotton, F. A.; Dunbar, K. R.; Lu, T.; Murillo, C. A.; Wang, X. *Inorg. Chem.* **2000**, *39*, 3065. (g) Clérac, R.; Cotton, F. A.; Daniels, L. M.; Dunbar, K. R.; Kirschbaum, K.; Murillo, C. A.; Pinkerton, A. A.; Schultz, A. J.; Wang, X. *J. Am. Chem. Soc.* **2000**, *122*, 6226. (h) Clérac, R.; Cotton, F. A.; Daniels, L. M.; Dunbar, K. R.; Murillo, C. A.; Wang, X. *J. Chem. Soc., Dalton Trans.*, **2001**, 386. (i) Clérac, R.; Cotton, F. A.; Daniels, L. M.; Dunbar, K. R.; Murillo, C. A.; Wang, X. *J. Am. Chem. Soc.* **2001**, *123*, 1256. (j) Clérac, R.; Cotton, F. A.; Jeffery, S. P.; Murillo, C. A.; Wang, X. *J. Am. Chem. Soc.* **2001**, *123*, 1265.
(9) Chang, H.-C.; Li, J.-T; Wang, C.-C.; Lin, T.-W.; Lee, H.-C.; Lee, G.-H.; Peng, S.-M. *Eur. J. Inorg. Chem.* **1999**, 1243.
(10) (a) Cotton, F. A.; Daniels, L. M.; Murillo, C. A.; Wang, X. *Chem. Commun.*, **1999**, 2461. (b) Cotton, F. A.; Daniels, L. M.; Murillo, C. A.; Wang, X. *J. Chem. Soc., Dalton Trans.*, **1999**, 517.
(11) Chen, Y.-H.; Lee, C.-C.; Wang, C.- C.; Lee, G.- H.; Lai, S.-Y.; Li, F.-Y.; Mou, C.-Y.; Peng, S.-M. *Chem. Commun.*, **1999**, 1667.
(12) (a) Rohmer, M.-M.; Strich, A.; Bénard, M.; Malrieu, J.-P. *J. Am. Chem. Soc.* **2001**, *123*, 9126. (b) Rohmer, M.-M.; Bénard, M. *J. Am. Chem. Soc.* **1998**, *120*, 9327.
(13) Crystal data for **[1]**·$4CH_2Cl_2$, formula $C_{64}H_{54}B_3Cl_8F_{12}N_{20}Ni_5O$, M_w = 1956.85, monoclinic, space group $P2_1/n$, T = 150(1) K, a = 15.3022(1), b = 31.0705(3), c = 15.8109(2) Å, β = 92.2425(4)°, V = 7511.49(13) Å^3, Z = 4, μ = 1.603 mm^{-1}, Dc = 1.730 g cm^{-3}. 52924 reflections collected, 17219 independent, R_{int} = 0.0732, final residuals $R1$ = 0.0773, $wR2$ = 0.2052 [$I>2\sigma(I)$]; $R1$ = 0.1322, $wR2$ = 0.2525 (all data). Crystal data for **[2]**·CH_2Cl_2·3.5(H_2O), formula $C_{64}H_{53}Cl_2F_9N_{20}Ni_5O_{12.5}S_3$, M_w = 1933.89, monoclinic, space group $C2/c$, T = 150(1) K, a = 42.1894(7), b = 17.0770(3), c = 21.2117(4) Å, β = 102.5688(8)°, V = 14916.1(5) Å^3, Z = 8, μ = 1.493 mm^{-1}, Dc = 1.722 g cm^{-3}. 46772 reflections collected, 13104 independent, R_{int} = 0.0868, final residuals $R1$ = 0.1065, $wR2$ = 0.2781 [$I>2\sigma(I)$]; $R1$ = 0.1605, $wR2$ = 0.3338 (all data)
(14) The molar magnetic susceptibility (χ^M) was fitted with the following equation using g = 2.41: $\chi^M = C(1+10e^{3x})/4(1+2e^{3x})$, where $C = Ng^2\beta^2/kT$ and $x = J/kT$.

Synopsis.

The one-electron oxidation products of the neutral pentanuclear nickel complex $[Ni_5(tpda)_4Cl_2]$ have been synthesized and structurally characterized. The Ni_5 unit of these oxidized complexes adopts an unsymmetrical structure and exhibits stronger metal-metal interactions as compared to the neutral analogues.

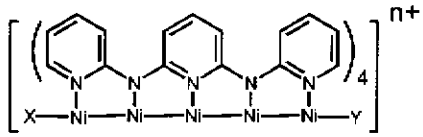

Ni—Ni	2.385	2.306	2.306	2.385	n = 0
Ni—Ni	2.337	2.261	2.245	2.300	n = **1**

The electrochemical properties of linear trichromium and tricobalt complexes with bis(2-pyridyl)amido ligands

Kun-Chih Pan,[a] Chen-Yu Yeh,[a] Chang-Ling Chiang,[a] Y. Oliver Su,*[a] Gene-Hsiang Lee[a] and Shie-Ming Peng*[ab]

[a] *Department of Chemistry, National Taiwan University, Taipei, Taiwan, ROC. Fax: 886-2-23691487; Tel: 886-2-23630231 ext. 3725; E-mail: smpeng@mail.ch.ntu.edu.tw*
[b] *Institute of Chemistry, Academia Sinica, Taipei, Taiwan, ROC.*

The electrochemical properties of $[Cr_3(dpa)_4Cl_2]$ and $[Co_3(dpa)_4Cl_2]$, where dpa is the anion of bis(2-pyridyl)amine, have been studied by cyclic voltammetry (CV) and spectroelectrochemistry. An electrochemical method has been developed to obtain the oxidized species of the trinuclear metal complexes by electrolysis. $[Cr_3(dpa)_4Cl_2]$ exhibits two reversible redox couples at $E_{1/2}$ = +0.18 and +0.95 V in CH_2Cl_2. The one-electron oxidation leads to an uncharacterized oxidized species $[Cr_3(dpa)_4XY]^+$ (X, Y = axial ligand) as major product and $[Cr_3(dpa)_4Cl_2]^+$ as minor product. The two-electron oxidized product is unstable and proceeds auto-reduction reaction to form $[Cr_3(dpa)_4Cl_2](ClO_4)$, which has been structurally characterized. $[Co_3(dpa)_4Cl_2]$ shows two reversible redox couples at $E_{1/2}$ = +0.43 and +1.34 V in CH_2Cl_2. One-electron oxidation generates a stable product and this product is characterized as $[Co_3(dpa)_4Cl_2](ClO_4)$. The X-ray crystal structures of $[Cr_3(dpa)_4Cl_2](ClO_4)$ and $[Co_3(dpa)_4Cl_2](ClO_4)$ generated by electrochemistry are comparable with those by chemical methods.

Introduction

Linear polynuclear metal complexes continue to attract much attention of inorganic chemists because of their fascinating chemistry such as spin interactions, metal-metal bonding, and their potential as molecular metalwires.[1-5] During the past decade, much effort has been devoted to the variation of metal centers, the increase of the chain length, the structural characterization, and the demonstration of the electronic configuration of these complexes. For instance, trinuclear metal complexes of Cr,[4] Co,[2,5] Ni,[6] Cu,[7] Rh[8] and Ru[8] wrapped by four bis(2-pyridyl)amido (dpa) ligands have been synthesized and structurally characterized, and their magnetic behavior has been described.

Among these trinuclear metal complexes, tricobalt and trichromium complexes are the most interesting ones since they exhibit both symmetrical and unsymmetrical structures depending on the nature of the axial ligands,[4] the crystal environment[5,9] and the oxidation states.[4,10] Despite the extensive studies on the structural characterization and magnetic properties of the compounds containing a trichromium or tricobalt core, the electrochemistry of these compounds has not been extensively investigated. We report here the electrochemical properties of $[Cr_3(dpa)_4Cl_2]$ and $[Co_3(dpa)_4Cl_2]$ along with the structures of their one-electron oxidized species obtained by electrochemical method. The schematic molecular structures of $[Cr_3(dpa)_4Cl_2]$ and $[Co_3(dpa)_4Cl_2]$ are given in Scheme 1.

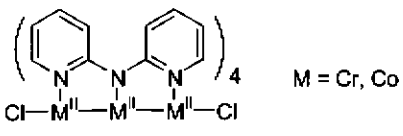

Scheme 1

Results and Discussion

Electrochemical Properties of $[Cr_3(dpa)_4Cl_2]$

The cyclic voltammograms of $[Cr_3(dpa)_4Cl_2]$ in CH_2Cl_2 are summarized in Figure 1. Two reversible redox couples occur at +0.18 and +0.95 V after 1 minute upon the addition of TBAP (Figure 1a). The couple at +0.95 V exhibits abnormal current magnitude and shape broadening. Most likely, it involves two species. A irreversible wave at –0.50 V is observed, the height of which increases, while the magnitude of the couple at +0.18 V decreases over time with addition of TBAP. A quasi-reversible peak at –0.73 V appears beyond the first reduction, the height of which increases upon decreasing the scan rate. This observation indicates that the reduction at –0.50 V is followed by a chemical reaction.

When TBAC instead of TBAP is used as the electrolyte, only one redox couple at +0.18 V is observed and the redox waves at +0.95 V (Figure 1a and 1b) are out of the breakdown limit in the solvent system. Furthermore, the irreversible cathodic current at –0.50 V in Figure 1b disappears. These observations indicate that there is a chemical reaction between $[Cr_3(dpa)_4Cl_2]$ and perchlorate, and the reaction produces a new complex. The irreversible reduction wave at –0.50 V in Figure 1b corresponds to the reduction of this newly formed complex. The formation of this new complex is observed by the UV-Vis spectral changes of $[Cr_3(dpa)_4Cl_2]$ in the presence of 1.0 M TBAP as shown in Figure 2. The resulting spectrum is identical with that of one-electron oxidation species obtained by electrolysis at $E_{appl.}$ = +0.5 V and is similar to those of $[Cr_3(dpa)_4F_2]^+$, $[Cr_3(dpa)_4(OH)(CF_3SO_3)]^+$ and $[Cr_3(dpa)_4(OH)(ClO_4)]^+$, which have already been structurally characterized.[11] The electrochemical and UV-Vis spectroelectrochemical characteristics of the new complex thus suggest that ligand exchange is followed by the one-electron oxidation, presumably leading to the new species, $[Cr_3(dpa)_4XY]^+$ (X = Y = ClO_4, or X = Cl and Y = ClO_4). Attempts to isolate and crystallize this product were unsuccessful.

As mentioned above, the second oxidation wave in Figure 1a and 1b could involve two species. This is evidenced by thin layer spectroelectrochemistry. About 10% of the one electron-oxidized species of $[Cr_3(dpa)_4Cl_2]$, obtained by electrolysis at +0.50 V, can be rereduced back to $[Cr_3(dpa)_4Cl_2]$ at +0.00 V, a potential at which $[Cr_3(dpa)_4XY]^+$ cannot be reduced. This indicates that during the one-electron oxidation, $[Cr_3(dpa)_4Cl_2]^+$ is the minor product, the amount of which is dependent on the electrolysis time. At the time scale of cyclic voltammetry, one-electron oxidation species, $[Cr_3(dpa)_4Cl_2]^+$, could coexist with $[Cr_3(dpa)_4XY]^+$, thus resulting in the broadening of the second

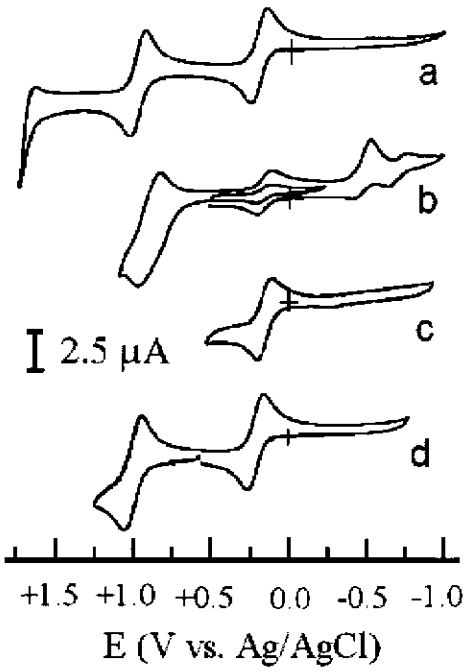

Fig. 1 The cyclic voltammograms of trichromium complexes in CH_2Cl_2. (a) $[Cr_3(dpa)_4Cl_2]$, 1 min after the addition of TBAP (0.1 M); (b) $[Cr_3(dpa)_4Cl_2]$, 30 min after the addition of TBAP (0.1 M); (c) $[Cr_3(dpa)_4Cl_2]$, electrolyte = 0.1 M TBAC; (d) $[Cr_3(dpa)_4Cl_2](ClO_4)$, 30 min after the addition of TBAP (0.1 M).

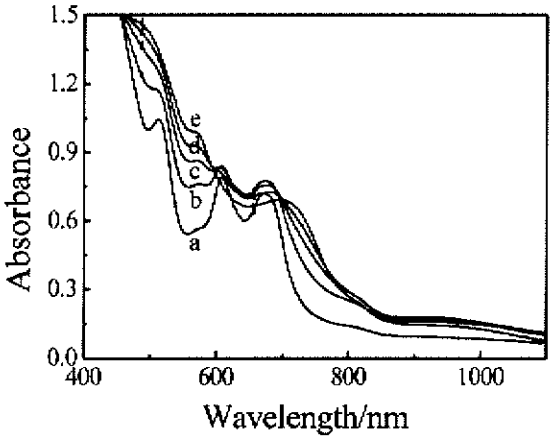

Fig. 2 UV-Vis spectral changes for the reaction between $[Cr_3(dpa)_4Cl_2]$ and 0.1 M TBAP in CH_2Cl_2. (a) freshly prepared; (b) 1; (c) 2; (d) 8; (e) 25; (f) 150 min after the addition of TBAP.

oxidation wave as shown in Figure 1b. These two one-electron oxidation species, upon further oxidation, lead to the same product as will be discussed later.

To further investigate the two electron-oxidized product of $[Cr_3(dpa)_4Cl_2]$, thin-layer UV-Vis spectroelectrochemistry was employed. After electrolysis at +1.25 V the two-electron oxidation species is obtained. The two-electron oxidized species is stable at the time scale of spectroelectrochemistry. However, attempts to isolate this oxidized species were unsuccessful. This oxidized species undergoes auto-reduction reaction to form a one-electron oxidation product as shown in Figure 3. The resulting spectrum of this auto-reduction reaction is identical

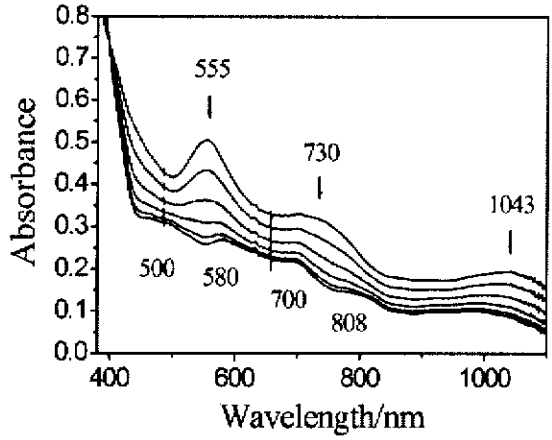

Fig. 3 UV-Vis spectral changes of auto-reduction of $[Cr_3(dpa)_4Cl_2]^{2+}$ obtained by electrolysis at +1.25 V in CH_2Cl_2 with 0.1 M TBAP. Time interval = 6 min.

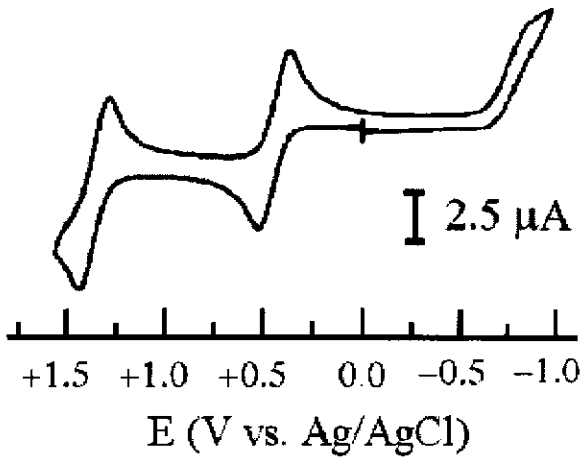

Fig. 4 The cyclic voltammograms of $[Co_3(dpa)_4Cl_2]$ in CH_2Cl_2 with 0.1 M TBAP.

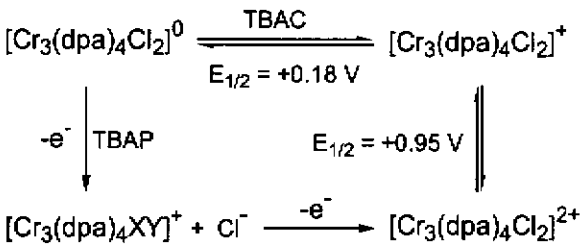

Scheme 2 The electrochemical oxidation pathways of $[Cr_3(dpa)_4Cl_2]$ in CH_2Cl_2 containing TBAP or TBAC.

with that of $[Cr_3(dpa)_4Cl_2]^+$ obtained by electrolysis at +0.5 V in CH_2Cl_2 containing 0.1 M TBAC. This auto-reduction product, $[Cr_3(dpa)_4Cl_2]^+$, is further characterized by the X-ray crystal structure. These results indicate that the two-electron oxidation species is $[Cr_3(dpa)_4Cl_2]^{2+}$.

To see whether or not $[Cr_3(dpa)_4Cl_2]^+$ can react with TBAP, we decided to study the electrochemical behavior of this

Table 1 Crystal data for $[Cr_3(dpa)_4Cl_2](ClO_4)$ and $[Co_3(dpa)_4Cl_2](ClO_4)$.

	$[Cr_3(dpa)_4Cl_2](ClO_4)$ ·1.75CH_2Cl_2·0.25($C_4H_{10}O$)	$[Co_3(dpa)_4Cl_2](ClO_4)$ ·2CH_2Cl_2
Formula	$C_{42.75}H_{38}Cl_{6.50}Cr_3N_{12}O_{4.25}$	$C_{42}H_{36}Cl_7Co_3N_{12}O_4$
FW	1174.28	1197.77
Crystal system	monoclinic	monoclinic
Space group	$P2_1/n$	$P2_1/n$
a, Å	11.5505(4)	11.4454(3)
b, Å	21.0962(7)	20.9334(5)
c, Å	19.8401(7)	19.6688(5)
β, deg	93.590(1)	92.499(1)
V, Å^3	4825.0(3)	4708.0(2)
F (000)	2380	2416
Crystal size (mm)	0.35 × 0.25 × 0.05	0.40 × 0.40 × 0.20
θ	1.41 to 27.50	1.42 to 27.50
Reflections	42383	43377
Absorption correction	multi-scan	multi-scan
Max and min trans	0.86 and 0.70	0.80 and 0.64
Refinement method	least-squares on F^2	least-squares on F^2
Z	4	4
T, K	150(1)	150(1)
D_{calc}, g/cm^3	1.617	1.690
Data/restraints/para	11072/8/621	10811/3/618
R_F, $R_w(F^2)$ (all data)[a]	0.1058, 0.1594	0.0357, 0.0941
R_F, $R_w(F^2)$ $[I > 2\sigma(I)]$[a]	0.0580, 0.1424	0.0553, 0.1002
GOF	1.048	1.067

[a] $R_F = \Sigma||F_o| - |F_c||/\Sigma|F_o|$; $R_w(F^2) = [\Sigma w|F_o^2 - F_c^2|^2/\Sigma w(F_o^4)]^{1/2}$.

oxidized species in CH_2Cl_2 containing 0.1 M TBAP. As shown in Figure 1d, two well-defined redox couples at +0.18 and +0.95 V are observed, indicating that there are no reactions between $[Cr_3(dpa)_4Cl_2]^+$ and TBAP. These results also provide strong evidence that the peak broadening at +0.95 V in Figure 1a is a result of the oxidation of $[Cr_3(dpa)_4XY]^+$.

According to the electrochemical and thin layer UV-Vis spectroelectrochemical results, the electrochemical reactions of $[Cr_3(dpa)_4Cl_2]$ is proposed in Scheme 2. In CH_2Cl_2 containing 0.1 M TBAP, ligand exchange is followed by a one-electron oxidation of $[Cr_3(dpa)_4Cl_2]$ to form a stable oxidized product, $[Cr_3(dpa)_4XY]^+$. However, the reaction of one-electron oxidation followed by ligand exchange cannot be ruled out. Further oxidation at +1.25 V gives a two-electron oxidation product, which can undergo auto-reduction reaction to form a stable one-electron oxidation species $[Cr_3(dpa)_4Cl_2]^+$.

Electrochemical Properties of $[Co_3(dpa)_4Cl_2]$

Figure 4 shows the cyclic voltammograms of $[Co_3(dpa)_4Cl_2]$ in CH_2Cl_2 containing 0.1 M TBAP. Two reversible redox couples at +0.44 and +1.34 V, and an irreversible wave at –0.75 V are observed. By judging from the peak currents, the two oxidation waves involve the same number of electrons. To investigate the stability of the oxidized species, thin layer UV-Vis spectroelectrochemistry is employed. Figure 5 shows the absorption spectra of $[Co_3(dpa)_4Cl_2]$ in CH_2Cl_2 at various potentials. As the applied potential increases, the peak at 568 nm shifts to 730 nm with a clear isosbestic point at 462 nm. The resulting spectrum is identical with that of $[Co_3(dpa)_4Cl_2]^+$ obtained by the reaction between $[Co_3(dpa)_4Cl_2]$ and $NOBF_4$.[9] According to the data obtained from spectroelectrochemistry, the formal potential of this electrochemical reaction is calculated to be +0.44 V and the number of electrons transferred is calculated to be 1.0. When the one-electron oxidation species is rereduced

Table 2 Comparison of Cr-Cr and Cr-Cl bond lengths (Å) in $[Cr_3(dpa)_4Cl_2](X)$[a].

X[a]	Cr(1)-Cr(2)	Cr(2)-Cr(3)	Cr(1)-Cl	Cr(3)-Cl
ClO_4	2.061(1)	2.492(1)	2.413(1)	2.303(1)
$AlCl_4$	2.010(1)	2.555(1)	2.441(2)	2.274(2)
$FeCl_4$	2.009(1)	2.562(1)	2.446(2)	2.278(2)
Cl	2.12(1)	2.47(1)	-	-
I_3	2.08(1)	2.49(1)	-	-
PF_6	2.09(2)	2.48(2)	-	-

[a] X = ClO_4, this work; X = $AlCl_4$, $FeCl_4$, Cl, I_3, and PF_6, see referece 4.

Table 3 Comparison of important bond lengths (Å) in $[Co_3(dpa)_4Cl_2](X)$ (X = ClO_4, BF_4).

	ClO_4	BF_4[a]
Co(1)-Co(2)	2.3214(4)	2.3168(8)
Co(2)-Co(3)	2.3311(4)	2.3289(8)
Co(1)-Cl	2.3674(7)	2.350(1)
Co(3)-Cl	2.3821(7)	2.376(1)
Co(1)-N	1.979(2)	1.975(4)
Co(2)-N	1.874(2)	1.869(4)
Co(3)-N	1.979(2)	1.979(4)

[a] reference 9.

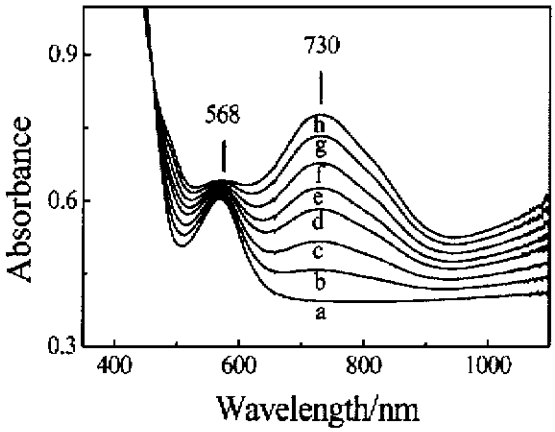

Fig. 5 UV-Vis Spectral changes of $[Co_3(dpa)_4Cl_2]$ during oxidation at various applied potentials from +0.25 to +0.51 V in CH_2Cl_2 with 0.1 M TBAP.

at +0.25 V, it can be completely converted back to $[Co_3(dpa)_4Cl_2]$. The one-electron oxidation species of $[Co_3(dpa)_4Cl_2]$ is characterized as $[Co_3(dpa)_4Cl_2](ClO_4)$, which is further confirmed by the X-ray crystal structure. Attempts to characterize the two-electron oxidation species of $[Co_3(dpa)_4Cl_2]$ were unsuccessful since it was unstable at the time scale of thin layer spectroelectrochemistry.

Electrolysis and Crystallization

The one-electron oxidation species $[Cr_3(dpa)_4Cl_2](ClO_4)$ can be obtained by auto-reduction of the two-electron oxidation product generated by bulk electrolysis in CH_2Cl_2 at +1.25 V. After the starting material is completely converted to the product as evidenced by UV-Vis spectroscopy, ether is slowly evaporated into the CH_2Cl_2 solution containing the oxidized compound. The crystals of the product and TBAP grow separately. High quality of crystals for X-ray crystallography is selected by hand. The crystals for analysis can be obtained by crystallizing twice from CH_2Cl_2 and ether. The other one-electron oxidation species, $[Cr_3(dpa)_4XY](ClO_4)$, can be obtained by employing a procedure similar to that described above after bulk electrolysis at +0.5 V in CH_2Cl_2. However, attempts to characterize this oxidized species were unsuccessful.

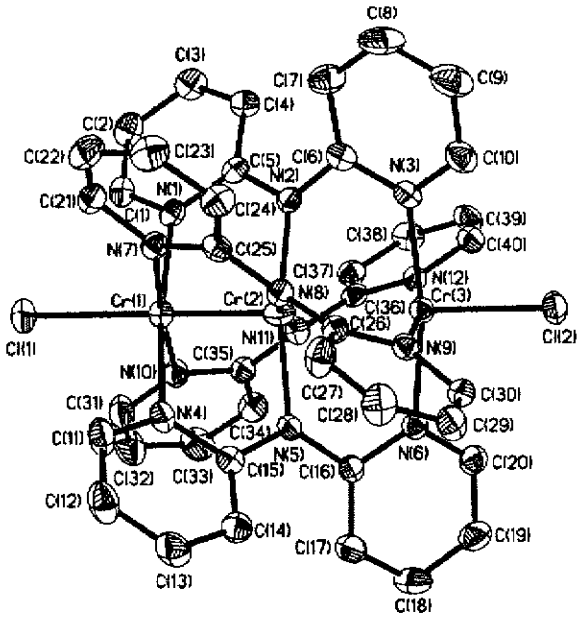

Fig. 6 The crystal structure of $[Cr_3(dpa)_4Cl_2]^+$. Atoms are drawn at the 50% probability level and hydrogen atoms are omitted for clarity.

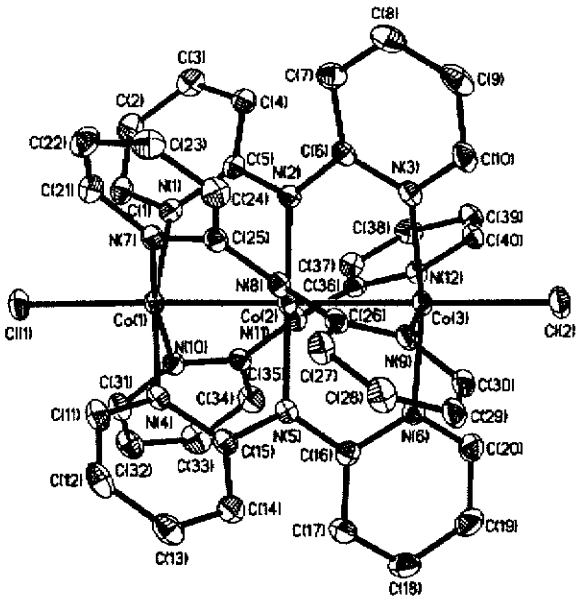

Fig. 7 The crystal structure of $[Co_3(dpa)_4Cl_2]^+$. Atoms are drawn at the 50% probability level and hydrogen atoms are omitted for clarity.

The synthesis of the one-electron oxidation compound of $[Co_3(dpa)_4Cl_2]$, in which the anion is tetraflouroborate, and its crystal structure have been reported. By using bulk electrolysis in CH_2Cl_2 at +0.75 V another one-electron oxidation form of $[Co_3(dpa)_4Cl_2]$, in which the anion is perchlorate, can be synthesized. High quality of crystals for X-ray crystallography can be obtained by employing a method similar to that for $[Cr_3(dpa)_4Cl_2](ClO_4)$.

Crystal Structure of $[Cr_3(dpa)_4Cl_2](ClO_4)$

The crystal structure of $[Cr_3(dpa)_4Cl_2](ClO_4)$ have not been previously reported. The detailed crystal data are listed in Tables 1. As shown in Figure 6, the core structure of $[Cr_3(dpa)_4Cl_2](ClO_4)$ is not significantly different from those reported by Cotton *et al.*[4] The selected bond distances along with those reported are listed in Table 2. This compound crystallizes in the $P2_1/n$ space group. The three Chromium atoms are in a linear arrangement helically wrapped by four dpa ligands. As expected, this molecule is unsymmetrical with Cr-Cr distances of 2.061(1) and 2.492(1) Å. The bond distances are consistent with the fact that Cr(1) and Cr(2) group up to form a quadruple bond, isolating Cr(3). The average Cr(1)-N distance is 2.111(4) Å, which is 0.027 Å longer than the Cr(3)-N distance. The Cr-Cl bond distances of 2.413(1) and 2.303(1) Å are comparable with those in $[Cr_3(dpa)_4Cl_2](FeCl_4)$ and $[Cr_3(dpa)_4Cl_2](AlCl_4)$. These bond distances are in a good agreement with Cr(1) and Cr(2) being Cr^{II}, and Cr(3) being Cr^{III}.

Crystal Structure of $[Co_3(dpa)_4Cl_2](ClO_4)$

Figure 7 shows the X-ray crystal structure of $[Co_3(dpa)_4Cl_2](ClO_4)$. The selected bond distances along with those reported[5] are listed in Table 3. This compound crystallizes in the $P2_1/n$ space group and isomorphous with that of $[Cr_3(dpa)_4Cl_2](ClO_4)$. The structure consists of a linear chain of three cobalt atoms supported by four dpa^{2-} ligands in a helical configuration and two chloride ions as the axial ligands. The positive charge is compensated by a perchlorate anion. The Co-Co-Co unit is symmetrical with Co(1)-Co(2) and Co(2)-Co(3) distances of 2.3214(4) and 2.3311(4) Å, respectively. The terminal Co-N bond distances are 1.979(2) for both Co(1) and Co(3). and the central Co-N bond distance is 1.874(2) Å. The average Cr-Cl bond length is 2.375(1) Å, significantly shorter than that of $[Co_3(dpa)_4Cl_2]$ (2.469(2) Å). All the bond distances described above are comparable with those in $[Co_3(dpa)_4Cl_2](BF_4)$ as listed in Table 3.

Conclusions

The electrochemical properties of $[Cr_3(dpa)_4Cl_2]$ and $[Co_3(dpa)_4Cl_2]$ have been demonstrated. The one-electron oxidation compounds of the trichromium and tricobalt complexes can be generated by bulk electrolysis and are sufficiently stable to be isolated. The structures of $[Cr_3(dpa)_4Cl_2]^+$ and $[Co_3(dpa)_4Cl_2]^+$ with perchlorate as the counter anion are compared with those of their analogues with different counter anions. Electrochemical methods have provided feasible means to prepare the single crystals of the oxidized species of linear trinuclear metal complexes and can be used for other multinuclear metal string complexes. Efforts along this line are underway in our laboratory.

Experimental Section

Materials

All reagents and solvents were obtained from commercial sources and were used without further purification unless otherwise noted. $[Co_3(dpa)_4Cl_2]$ was prepared according to previously reported procedures from the literatures.[2a] CH_2Cl_2 used for electrochemistry was dried over CaH_2 and freshly distilled prior to use. Tetra-*n*-butylammonium perchlorate (TBAP) and tetra-*n*-butylammonium chloride (TBAC) were each recrystallized twice from ethyl acetate and toluene, respectively, and further dried under vacuum.

Physical Measurements

Absorption spectra were recorded on a Hewlett Packard model 8453 spectrophotometer. IR spectra were performed with a Nicolet Fourier-Transform IR or MAGNA-IR 500 spectrometer in the range of 500-4000 cm^{-1}. FAB-MS mass spectra were obtained with a JEOL HX-110 HF double focusing spectrometer operating in the positive ion detection mode. Electrochemistry

was performed with a three-electrode potentiostat (Bioanalytical Systems, Model CV-27) and a BAS X-Y recorder in a CH_2Cl_2 solution deoxygenated by purging with prepuried nitrogen gas. Cyclic voltammetry was conducted with the use of a home-made three-electrode cell equipped with a BAS glassy carbon (0.07 cm^2) or platinum (0.02 cm^2) disk as the working electrode, a platinum wire as the auxiliary electrode, and a home-made Ag/AgCl (sat'd) reference electrode. The reference electrode is separated from the bulk solution by a double junction filled with electrolyte solution. Potentials are reported vs. Ag/AgCl (sat'd) and referenced to the ferrocene/ferrocenium (Fc/Fc^+) couple which occurs at $E_{1/2}$ = +0.54 V vs. Ag/AgCl (sat'd). The working electrode was polished with 0.03 μm aluminum on Buehler felt pads and was ultrasonicated for 1 min prior to each experiment. The reproducibility of individual potential values was within ±5 mV. The spectroelectrochemical experiments were accomplished with the use of a 1 mm cuvette, a 100 mesh platinum gauze as working electrode, a platinum wire as auxiliary electrode, and a Ag/AgCl (sat'd) reference electrode. The design of cuvettes for spectroelectrochemical measurements has been described.[12] A two-arm U-shape cell with a fritted-glass separator was used for bulk electrolysis. The cell is equipped with platinum gauzes as working and auxiliary electrodes, and a Ag/AgCl (sat'd) reference electrode, which is placed close to the working electrode.

Preparation of Compounds

$[Cr_3(dpa)_4Cl_2]$. Anhydrous $CrCl_2$ (0.37 g, 3.0 mmole), dipyridylamine (0.68 g, 4.0 mmole) and naphthalene (20 g) were placed in an Erlenmeyer flask. The mixture was gently refluxed under an argon atmosphere for 4 hr. A solution of potassium *t*-butoxide (0.45g, 4.0 mmole) in *t*-butanol (5 mL) was added dropwise. The resulting solution was further refluxed for 2 hr until it turned a dark green. After the mixture had cooled, hexane (100 mL) was added and the precipitate was filtered. The solid was extracted with CH_2Cl_2 and crystallized from CH_2Cl_2 and ether to give 0.68 g of deep brown crystals (75%). IR (KBr) ν/cm^{-1} = 1605, 1594, 1547 (pyridyl); UV/Vis (CH_2Cl_2) λ_{max}/nm ($\varepsilon/dm^3\ mol^{-1}\ cm^{-1}$) = 230 ($2.91 \times 10^4$), 292 ($3.66 \times 10^4$), 608 ($1.44 \times 10^3$), 672 ($1.29 \times 10^3$); MS(FAB) m/z 906 ($[Cr_3(dpa)_4Cl_2]^+$), 871 ($[Cr_3(dpa)_4Cl]^+$). EA (%) $[Cr_3(dpa)_4Cl_2]\cdot(CH_2Cl_2)\cdot(C_4H_{10}O)$: calcd. C 51.30, H 4.12, N 15.62; found C 51.46, H 4.21, N 16.43.

$[Cr_3(dpa)_4Cl_2](ClO_4)$. A solution of $[Cr_3(dpa)_4Cl_2]$ (100 mg) in CH_2Cl_2 (20 mL) containing 0.1 M TBAP was electrolyzed at $E_{appl.}$ = +1.25 V vs. Ag/AgCl. The reaction was monitored by UV/Vis spectroscopy. After the reaction was complete (about 60 min), the solution was concentrated under reduced pressure. Deep brown crystals were obtained by slow evaporation of ether into the concentrated CH_2Cl_2 solution. Samples for analysis were crystallized twice from CH_2Cl_2 and ether (80 mg, 72%). IR (KBr) ν/cm^{-1} = 1609, 1601, 1562 (pyridyl); UV/Vis (CH_2Cl_2) λ_{max}/nm ($\varepsilon/dm^3\ mol^{-1}\ cm^{-1}$) = 295 ($4.72 \times 10^4$), 496 ($2.62 \times 10^3$), 578 ($2.46 \times 10^3$), 692 ($1.97 \times 10^3$), 795 ($1.10 \times 10^3$); MS(FAB) m/z 906 ($[Cr_3(dpa)_4Cl_2]^+$), 871 ($[Cr_3(dpa)_4Cl]^+$); EA (%) $[Cr_3(dpa)_4Cl_2](ClO_4)\cdot 2CH_2Cl_2\cdot 2H_2O$: calcd. C 41.59, H 3.32, N 13.86; found C 41.65, H 3.38, N 14.23.

$[Co_3(dpa)_4Cl_2](ClO_4)$. A solution of $[Co_3(dpa)_4Cl_2]$ (100 mg) in CH_2Cl_2 (20 mL) containing 0.1 M TBAP was electrolyzed at $E_{appl.}$ = +0.80 V vs. Ag/AgCl. The reaction was monitored by UV/Vis spectroscopy. After the reaction was complete, the solution was concentrated under reduced pressure. Dark green crystals were obtained by slow evaporation of ether into the concentrated CH_2Cl_2 solution. Samples for analysis were crystallized twice from CH_2Cl_2 and ether (84 mg, 76%). IR (KBr) ν/cm^{-1} = 1603, 1574, 1562, 1552 (C=C); UV/Vis (CH_2Cl_2) λ_{max}/nm ($\varepsilon/dm^3\ mol^{-1}\ cm^{-1}$) = 305 ($5.10 \times 10^4$), 434 ($6.20 \times 10^3$), 724 ($3.76 \times 10^3$); MS(FAB) m/z 927 ($[Co_3(dpa)_4Cl_2]^+$), 892 ($[Co_3(dpa)_4Cl]^+$); EA (%) $[Co_3(dpa)_4Cl_2](ClO_4)\cdot CH_2Cl_2\cdot H_2O$: calcd. C 43.55, H 3.21, N 14.86; found C 43.54, H 3.28, N 15.16.

Crystal Structure Determinations

The chosen crystals were mounted on a glass fiber. The diffraction data were collected on a Bruker SMART diffractometer equipped with a CCD detector, a Mo radiation (λ = 0.71073 Å), and a liquid nitrogen low-temperature controller. For each structure, data were measured using ω scans of 0.3° per frame for 5 and 10 s for $[Co_3(dpa)_4Cl_2](ClO_4)$ and $[Cr_3(dpa)_4Cl_2](ClO_4)$, respectively, until a complete hemisphere had been collected. Cell parameters were retrieved using SMART software[13] and refined with SAINT on all observed reflections. Data reduction was performed with the SAINT software[14] and corrected for Lorentz and polarization effects. Absorption corrections were applied with the program SADABS.[15] The detailed crystal data are listed in Table 1.

Acknowledgment

The authors thank the National Science Council of the Republic of China for financial support.

References

1 A. Name, B. Name and C. Name, *Journal Title*, 2000, **35**, 3523; A. Name, B. Name and C. Name, *Journal Title*, 2000, **35**, 3523.
1 H.-C. Chang, J.-T Li, C.-C. Wang, T.-W. Lin, H.-C. Lee, G.-H. Lee and S.-M. Peng, *Eur. J. Inorg. Chem.*, 1999, 1243; Y.-H. Chen, C.-C. Lee, C.-C. Wang, G.- H. Lee, S.-Y. Lai, F.-Y. Li, C.-Y. Mou and S.-M. Peng, *Chem. Commun.*, 1999, 1667.
2 E.-C. Yang, M.-C. Cheng, M.-S. Tsai and S.-M. Peng, *J. Chem. Soc., Chem. Commun.*, 1994, 2377; S.-J. Shieh, C.-C. Chou, G.-H. Lee, C.-C. Wang and S.-M. Peng, *Angwe. Chem. Int. Ed. Engl.*, 1997, **36**, 56.
3 C.-C. Wang, W.-C. Lo, C.-C. Chou, G.-H. Lee, J.-M. Chen and S.-M. Peng, *Inorg. Chem.*, 1998, 4059; S.-Y. Lai, T.-W. Lin, Y.-H. Chen, C.-C. Wang, G.-H. Lee, M.-H. Yang, M.-K. Leung and S.-M. Peng, *J. Am. Chem. Soc.*, 1999, **121**, 250.
4 R. Clérac, F. A. Cotton, L. M. Daniels, K. R. Dunbar, C. A. Murillo and I. Pascual, *Inorg. Chem.*, 2000, **39**, 748; R. Clérac, F. A. Cotton, L. M. Daniels, K. R. Dunbar, C. A. Murillo and I. Pascual, *Inorg. Chem.*, 2000, **39**, 752.
5 F. A. Cotton, L. M. Daniels and G. T. Jordan IV, *Chem. Commun.*, 1997, 421; R. Clérac, F. A. Cotton, L. M. Daniels, K. R. Dunbar, K. Kirschbaum, C. A. Murillo, A. A. Pinkerton, A. J. Schultz and X. Wang, *J. Am. Chem. Soc.*, 2000, **122**, 6226; F. A. Cotton, C. A. Murillo and X. Wang, *Inorg. Chem.*, 1999, **38**, 6294; F. A. Cotton, L. M. Daniels, G. T. Jordan IV and C. A. Murillo, *J. Am. Chem. Soc.*, 1997, **119**, 10377.
6 S. Aduldecha and B. Hathaway, *J. Chem. Soc., Dalton. Trans.*, 1991, 993.
7 G. J. Pyrka, M. El-Mekki and A. A. Pinkerton, *J. Chem. Soc., Chem. Commun.*, 1991, 84; L.-P. Wu, P. Field, T. Morrissey, C. Murphy, P. Nagle, B. Hathaway, C. Simmons and P. Thornton, *J. Chem. Soc., Dalton. Trans.*, 1990, 3835.
8 J.-T. Sheu, C.-C. Lin, I. Chao, C.-C. Wang and S.-M. Peng, *Chem. Commun.*, 1996, 315.
9 R. Clérac, F. A. Cotton, L. M. Daniels, K. R. Dunbar, C. A. Murillo and X. Wang, *J. Am. Chem. Soc.*, 2001, **123**, 1256; R. Clérac, F. A. Cotton, L. M. Daniels, K. R. Dunbar, T. Lu, C. A. Murillo and X. Wang, *J. Am. Chem. Soc.*, 2000, **122**, 2272.
10 F. A. Cotton, L. M. Daniels, C. A. Murillo and I. Pascual, *J. Am. Chem. Soc.*, 1997, **119**, 10223.
11 The structure of $[Cr_3(dpa)_4(OH)(ClO_4)](ClO_4)$ will be published elsewhere.
12 X. H. Mu and K. M. Kadish, *Inorg. Chem.*, 1988, **27**, 4720.
13 *SMART V 4.043 Software for The CCD Detector System*; Siemens Analytical Instruments Division: Madison, WI, 1995.
14 *SAINT V 4.035 Software for the CCD Detector System*; Siemens Analytical Instruments Division, Madison, WI, 1995.
15 G. M. Sheldrick, *SHELXL-93, Program for the Refinement of Crystal Structures*; University of Göttingen, Göttingen, Germany, 1993.

Synopsis

The electrochemical properties of linear trichromium and tricobalt complexes with bis(2-pyridyl)-amido ligands

Kun-Chih Pan, Chen-Yu Yeh, Chang-Ling Chiang, Y. Oliver Su, Gene-Hsiang Lee and Shie-Ming Peng

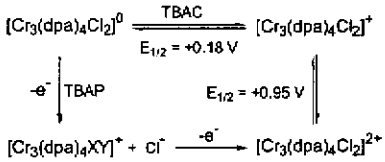

The electrochemical properties of $[Cr_3(dpa)_4Cl_2]$ and $[Co_3(dpa)_4Cl_2]$ have been studied, and electrochemical methods have been developed to obtain the oxidized species of these trinuclear metal complexes.